Gas permeation through water-swollen sericin / PVA membranes

by

Se Jin Kim

A thesis
presented to the University of Waterloo
in fulfillment of the
thesis requirement for the degree of
Master of Applied Science
in
Chemical Engineering

Waterloo, Ontario, Canada, 2007

I hereby declare that I am the sole author of this thesis.

This is a true copy of the thesis, including any required final revisions, as accepted by my examiners.

I understand that my thesis may be made electronically available to the public.

Abstract

Silk sericin, a protein obtained from cocoons, is a highly hydrophilic macromolecular material with many hydroxyl, carboxyl and amino acid groups. Sericin has been used for cosmetics, medical, polymer materials and other applications due to its antioxidative, antibacterial, UV resistant and moisture-absorbing and -desorbing properties. On the other hand, polyvinyl alcohol (PVA) has been used as a membrane material because of its good film forming properties. In this study, sericin was blended with PVA to form membranes that are permselective to gases. Due to their hydrophilic properties a novel water-swollen sericin / PVA membrane was investigated for the gas permeation of carbon dioxide and nitrogen.

Silk sericin with molecular weights 26 - 170 kDa was obtained from cocoons by extraction with water. At $95\,^{\circ}C$ the yield of sericin was found to be 22.8% after 9 hrs of extraction. The sericin / PVA membranes were prepared by blending sericin and PVA followed by crosslinking with glutaradehyde. After drying, the membranes were heat treated at $120\,^{\circ}C$ for 1 hr. The membranes containing 0 to 30.3% sericin showed that the permeability was 2.7-4.0 Barrer for O_2, 1.3-2.3 Barrer for N_2 and 66.5- 28.8 Barrer for CO_2, corresponding to a separation factor in the range of 48.3 to 60 for CO_2/N_2 and 1.4 to 2.2 for O_2/N_2. The membranes showed a favourable selectivity for CO_2/N_2 separation, which is relevant to CO_2 capture from flue gas for green house gas emission control.

In addition, the effects of water in the membrane on the membrane properties were evaluated. It was shown that the swelling of the membranes with water tended to

improve the permeability and selectivity of the membranes due to the increased free volume available for gas transport in the membrane. The water vapor sorption and desorption were also studied, and the diffusion coefficient was determined. It was found that the membrane permeability depended on the water sorption uptake in water-swollen membranes.

Acknowledgements

It is my pleasure to thank my supervisor Professor X. Feng for his guidance, valuable comments and expert suggestions throughout the research work and the preparation of this thesis for my Master's program.

I also would like to thank Eddie, Jennifer, Li, Andy, Mujib and Elaine, my fellow graduate students in the Membrane Research lab, who were always helping and encouraging me in my research. It was such a great time to be with my Korean friends, Faith Park, Hyuk Sang Park, Sang Young Shin, Yi Young Choi, Woosung Jung and Seung Mi Yoo, who were giving me their warm hearts and happiness. The time I spent with them will be precious and unforgettable.

It is glad to thank my family and friends in Korea for their care and financial support with their priceless love. Through my master program and living far from my country I realize how significant they are in my life.

The silk worm cocoon sample was kindly provided by Dr. Marcelino Gimenes, State University of Maringa, Brazil. Research support from the Natural Sciences and Engineering Research Council (NSERC) of Canada is gratefully acknowledged.

Table of contents

List of tables

List of figures

Chapter 1

Introduction

Greenhouse effect is nowadays a big issue with a worldwide concern due to water vapor and carbon dioxide gas, which cause global warming of the earth, from different emission sources, particularly from flue gas in power stations, steel works and chemical industries. Because of their molecular structures theses gases absorb mainly reflected solar radiation from the earth's surface so that the heat at atmosphere is entrapped. Interest in the separation and recovery of carbon dioxide has increased to develop clean and energy-efficient separation processes since the production of carbon dioxide, a major component among the greenhouse gases, is an environmental issue worldwide. The use of polymeric gas separation membranes can be applied to separate carbon dioxide from flue gas.

Gas separation is a major operation in the chemical industry, and the oxygen/nitrogen separation is one of the main applications. In many industrial processes oxygen enriched air is required for, e.g. combustion of natural gas, coal gasification, as well as in the production of peroxides, in sewage treatment and glass production.

Traditional methods are cryogenic distillation and pressure swing adsorption. Due to the highly intensive energy cost of these techniques, a less costly process is required. As an alternative process, membrane gas separation for the production of oxygen enriched air has been investigated over the last 30 years based on polymeric membranes and carrier mediated transport. Although polymeric membranes systems have been proven to be less cost intensive to operate, they are still not suitable to produce highly oxygen enriched air, i.e. air with an oxygen content in excess of 50-60 vol.% for large scale commercial production. [1]

Membrane gas separation has become a remarkable industrial application of membrane technology during the past three decades. It offers a number of advantages in terms of energy consumption and capital cost. The process equipment is simple, compact, and relatively easy to operate and control. In order to be used economically, the membrane performance should exhibit high permeability and selectivity for the components to be separated. However, permeability and selectivity of common polymeric membranes are generally inversely related. Typical nonporous polymeric membranes exhibit CO_2/CH_4 and CO_2/N_2 selectivities around 15-35. [2]

To improve the permeability and/or selectivity, facilitated transport mechanism was studied. For the case of facilitated carbon dioxide transport (See Figure 1-1), the carrier is specific to carbon dioxide. The carrier is dissolved into the membrane to preferentially permeate carbon dioxide over nitrogen. As a result, the flux of carbon dioxide is enhanced which results in a higher carbon dioxide concentration on the permeate side. The transport of carbon dioxide through facilitated membranes can be considered to be a 3 step process: First, carbon dioxide and the carrier present in the membrane form a complex at the feed side. Then, the CO_2-carrier complex diffuses

through the membrane. Finally, carbon dioxide is released to the permeate side, and the carrier is restored or regenerated to its original forms. A detailed discussion with an example of oxygen facilitated transport mechanism is reviewed in Section 2.1.3.

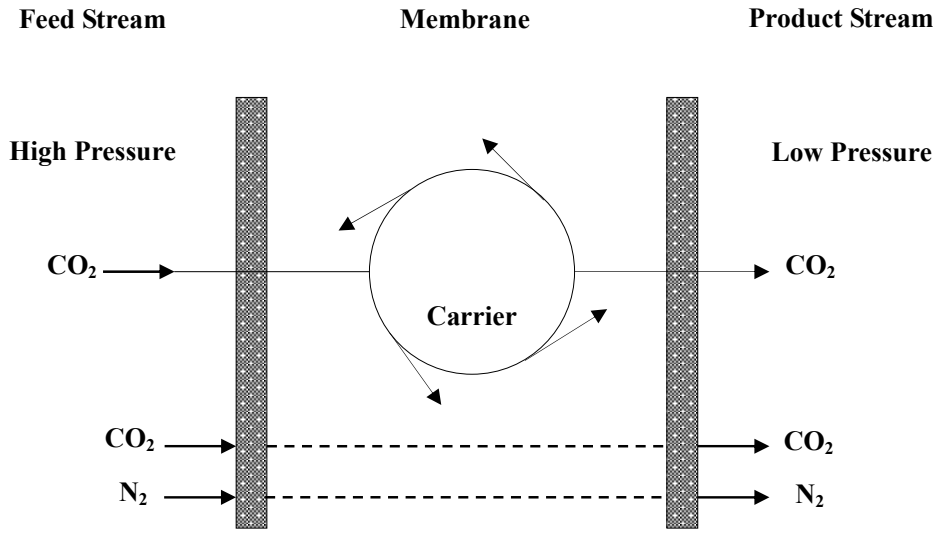

Figure 1-1 Facilitated transport of CO_2 in the presence of a carrier in the membrane, along with transport of CO_2 and N_2 by ordinary solution-diffusion mechanism

In this study, a novel membrane comprising of sericin and polyvinyl alcohol (PVA) was investigated for the permeation of carbon dioxide, oxygen and nitrogen. By using water-swollen membranes, the gas permeability is expected to be higher than a dry membrane because of the flexible polymer chains and large free volume in water-wet state. [3] Silk sericin is a protein obtained from cocoons by extraction with boiling water and it is a highly hydrophilic macromolecular material due to its many hydroxyl, carboxyl, and amino acid groups. Thus, silk sericin was used in this study to make polymeric membranes. On the other hand, PVA also has many hydroxyl groups so that it was easy to make water-swollen membranes with both materials because of their

hydrophilic properties. Water-swollen sericin / PVA membranes were prepared, and the membrane properties were evaluated for carbon dioxide, oxygen and nitrogen permeation. By measuring water swelling ratio and water vapor sorption/desorption it was found that the effect of water on membrane was related with the gas permeation rates.

The specific objectives of this study are to:

1. Select a suitable extraction method for silk sericin from the silkworm cocoons.
2. Choose a suitable membrane system in terms of sericin and PVA composition.
3. Evaluate the membrane properties by conducting gas permeation experiments.
4. Analyze the results from the gas permeation experiments.
5. Evaluate the water effect on membranes by measuring water swelling ratio and water vapor sorption/desorption in the sericin / PVA membranes.

This thesis work will address the following aspects:

Chapter 1 gives an introduction of this research. The basis of membrane gas separation and objectives of this study are briefly introduced.

Chapter 2 reviews the background of membrane gas separation and transport mechanisms of membrane process. This chapter also reviews the background of silk sericin.

Chapter 3 deals with the extraction of silk sericin, and membrane preparation. The experimental procedure for gas permeation is described, and the characterization of membrane property is introduced.

Chapter 4 presents and discusses the experimental results.

Finally, the conclusions drawn from this study and recommendations for future work are presented in Chapter 5. Moreover, sample calculations and raw data are presented in the appendix.

Chapter 2

Literature review and background

Membrane gas separation process is an important unit operation widely employed in the chemical industries. Membrane-based gas separation offers a number of advantages compared to other traditional methods for certain applications. Most notable features of membrane processes are low capital and operating costs, low energy requirements, and moderate operating conditions. Membrane gas separation appeared as a commercial process on a large scale during the 1980s. Since then, significant progress has been made in membrane technology, including improvements in membrane formation processes, chemical and physical structures, and applications. Table 2-1 lists the current status of membrane gas separation processes. The established processes represent more than 80% of the current gas separation membrane market: nitrogen production from air, hydrogen recovery and air drying. All have been used on a large commercial scale for over 10 years with dramatic improvements in membrane selectivity, flux and process designs. The second group of applications is developing processes which include carbon dioxide separation from natural gas, organic vapor separation from air and nitrogen, and recovery of light hydrocarbons from refinery and

Table 2-1 Status of membrane gas separation processes [4]

Process	Application	Comments
Established processes		
Oxygen/nitrogen	Nitrogen from air	Processes are all well developed. Only incremental improvements in performance expected
Hydrogen/methane; hydrogen/nitrogen; hydrogen/carbon monoxide	Hydrogen recovery; ammonia plants and refineries	
Water/air	Drying compressed air	
Developing processes		
VOC/air	Air pollution control applications	Several applications being developed. Significant growth expected as the process becomes accepted
Light hydrocarbons from nitrogen or hydrogen	Reactor purge gas, petrochemical process streams, refinery waste gas	Application is expanding rapidly
Carbon dioxide/methane	Carbon dioxide from natural gas	Many plants installed but better membranes are required to change market economics significantly
To be-developed processes		
C_{3+} hydrocarbons/methane	NGL recovery from natural gas	Field trials and demonstration system tests under way. Potential market is large
Hydrogen sulfide, water/methane	Natural gas treatment	Niche applications, difficult for membranes to compete with existing technology
Oxygen/nitrogen	Oxygen enriched air	Requires better membranes to become commercial. Size of ultimate market will depend on properties of membranes developed. Could be very large
Organic vapor mixtures	Separation of organic mixtures in refineries and petrochemical plants	Requires better membranes and modules. Potential size of application is large

petrochemical plant purge gases. Theses processes are being developed on a commercial scale, and the process performance has been improved with the development of better membranes and process designs. In addition, organic vapor separation membranes are currently being developed for petrochemical and refinery applications. The 'to be developed' membrane processes represent the future development of gas separation technology. Natural gas treatment by membranes is being carried out at field tests and early commercial stage by several companies. Another large potential application for membranes is the production of oxygen-enriched air, and the market size is expected to depend largely on the properties of the membranes. [4]

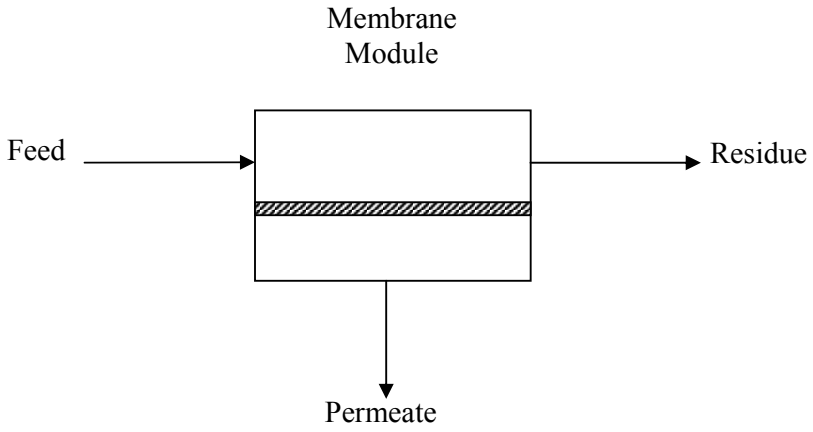

Figure 2-1 Schematic diagram of the basic membrane gas separation process

2.1 Transport mechanism

The membrane can be simply defined as a permselective barrier that will favor the transport of one component over the others. The separation occurs as a result of the differences in permeabilities of the species through the membrane. In gas separation, when a gas mixture at a pressure higher than the other side contacts a membrane which is selectively permeable to one component of the feed mixture, that species will be

enriched on the permeate side. The basic process of gas separation membranes is illustrated in Figure 2-1. In general, as shown in Figure 2-2, gas separation can be performed using membranes based on one of the mechanisms. There are generally two types of membranes: porous and dense membranes. Both porous and dense membranes can be used as selective gas separation barriers, although porous membranes are normally not selective enough for efficient separations.

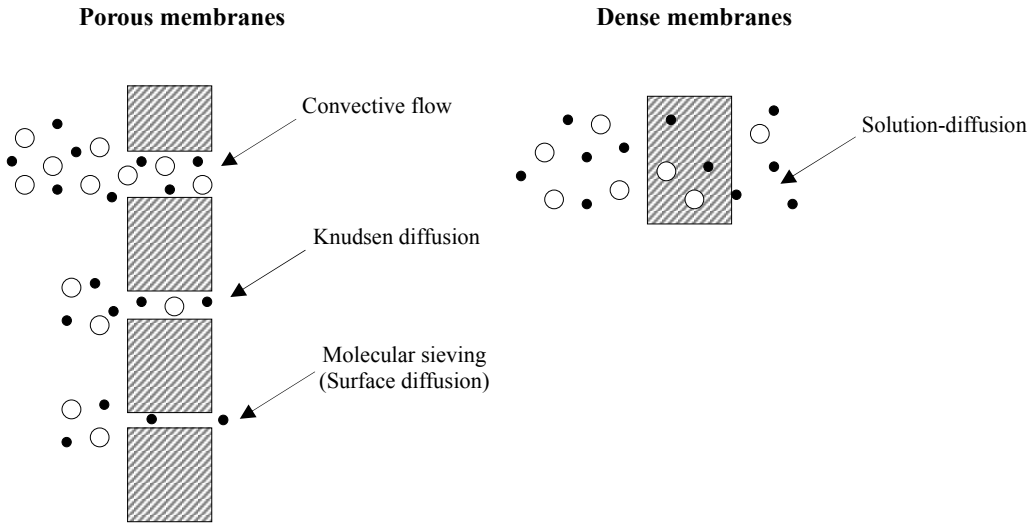

Figure 2-2 Mechanisms for permeation of gases through porous and dense membranes [4]

In porous membranes, three different transport mechanisms may occur depending on the pore size. If the pores are relatively large (0.1 to 10 μm), separation does not occur and gases permeate across the membrane by convective flow. When the mean free path of the gas molecules is same as or greater than the pore size, Knudsen diffusion takes place. In this transport mechanism, the collisions of the gas molecules with the pore wall are more frequent than the collisions among molecules. The transport rate of the gas through the pores is inversely proportional to the square root of its molecular weight. This relationship is called Graham's law of diffusion. When the pores are

extremely small, the feed gases are separated by molecular sieving, and large molecules can hardly pass through the membrane. This type of mechanism is complex due to the diffusion in the gas phase and the diffusion of adsorbed species on the surface of the pores, and such membranes have not been used on a large scale. [4, 5]

2.1.1 Solution-diffusion mechanism

The mechanism of gas separation by dense membranes is quite different. In dense polymeric membranes, solution-diffusion is generally accepted to be the main mechanism of transport. Moreover, these membranes are commercially available. An important feature of dense membranes is the ability to control the permeation of different species. Based on solution-diffusion mechanism, gas permeation is generally considered to be a three-step process : [6]

(1) The gas molecules are sorbed on the membrane surface at the upstream side,

(2) The sorbed gas molecules diffuse through the polymer to the downstream side,

(3) The gas molecules desorb on the downstream side.

2.1.2 Theory of gas transport through membranes

In this section a simplified development of the gas transport theory across a membrane is discussed. To simplify, pure gas permeation is considered. The total flux of a gas across the membrane can be expressed by Fick's first law:

$$J = -D\left(\frac{dC}{dx}\right) \tag{2.1}$$

where D is the diffusion coefficient and dC/dx is the concentration gradient of the gas through the membrane. The flux is a constant at steady state. Equation (2.1) can be

integrated, if D is assumed to be constant, to give

$$J = D\frac{C_p - C_f}{l} \tag{2.2}$$

where C_p and C_f are the concentration of the gas in the membrane on the feed and permeate sides, respectively, and l is the thickness of the membrane. The concentration of the gas in the membrane can be expressed by the Henry's law:

$$C = Sp \tag{2.3}$$

where S is the solubility coefficient and p is the gas pressure. Combining equations (2.2) and (2.3), the flux can be presented in terms of the diffusion and solubility coefficients:

$$J = DS\frac{p_f - p_p}{l} = P\frac{p_f - p_p}{l} \tag{2.4}$$

where P is permeability of the gas defined as:

$$P = DS \tag{2.5}$$

The permeability is a product of the diffusivity and solubility coefficients. Thus, it can be seen that two parameters describe the solution-diffusion model: solubility and diffusivity. The permeability is a product of a thermodynamic factor (the solubility coefficient S) and a kinetic parameter (the diffusion coefficient D). In real systems, both diffusion and solubility coefficients may be a function of concentration.

Selectivity is defined by the ratio of the individual gas permeabilities. Based on pure gas permeabilities, the "ideal selectivity" for gas species "A" and "B" can be defined as:

$$\alpha_{AB} = \frac{P_A}{P_B} = \left(\frac{D_A}{D_B}\right)\left(\frac{S_A}{S_B}\right) \tag{2.6}$$

which shows that the overall selectivity is determined by the differences in both the diffusivity and solubility coefficients, and measure the contributions of diffusivity and solubility aspects of the gas permeation, respectively.

2.1.3 Facilitated transport mechanism

Facilitated transport is a promising approach to enhancing permeability and selectivity with long-term durability. However, the membrane instability with the commonly used facilitated transport liquid membranes is a major obstacle for industrial applications. Two types of transport can be distinguished: mobile and fixed carriers. Facilitated transport is a coupled transport process which can be described with a (chemical) coupling reaction and a diffusion process. Firstly, the solute reacts with the carrier to form a solute-carrier complex. Then it diffuses across the membrane to release the solute at the permeate side. The entire process can be considered as a passive transport because the solute molecules are transported under the chemical potential gradient. In the case of solid membranes with fixed carriers, the carrier can be chemically or physically bound to the membrane, whereby the solute hops from one site to the other. In immobilized liquid membranes with mobile carriers which consist of a solid membrane (support) and a liquid phase containing the carrier molecules, the carrier molecules function as a shuttle to transport the solute from feed side to the permeate side. Figure 2-3 is a schematic showing the facilitated transport with mobile and fixed carriers in the membranes. [1]

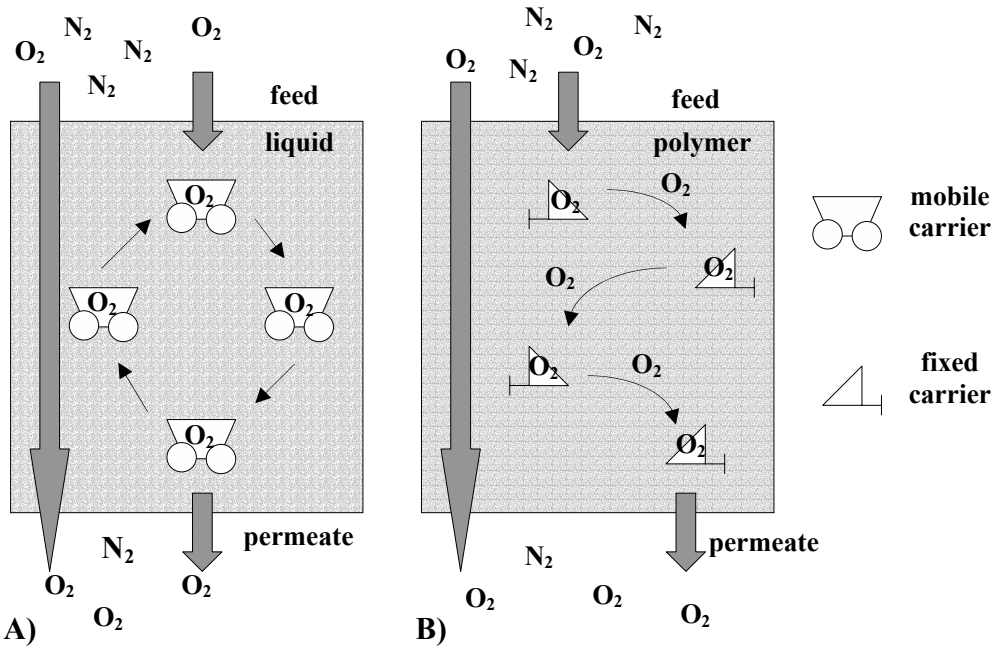

Figure 2-3 Facilitated transport of gaseous molecules: (A) liquid membrane with a mobile carrier; (B) solid membrane with a fixed carrier. [1]

Both types of facilitated transport systems are sometimes referred to as dual-mode transport, which was first proposed to explain the transport of gases, such as carbon dioxide, in glassy polymers. The solution-diffusion transport is one mode of transport through the membrane. The second mode concerns with chemical facilitation of permeation. Thus, the total flux is not proportional to the driving force because of the dual mechanisms. [1]

The facilitated transport membranes can be used to improve the selectivity and permeation flux. However, as shown in Table 2-2, where the requirements, advantages and disadvantages of both types of carrier systems are listed, there are some problems related to the loss of solvent and carrier, and temperature limitations.

Table 2-2 The pre-requisites, advantages and disadvantages of mobile and fixed carrier facilitated transport systems with respect to oxygen permeation [1]

	Mobile carrier (liquid)	**Fixed carrier** (polymer film)
Requirements	**Membrane**: low effective thickness **Liquid medium**: low viscosity, low volatility, high compatibility with polymeric material **Carrier**: high concentration in the liquid medium, high selectivity for O_2	**Membrane**: low thickness **Carrier**: high concentration in the polymer matrix, high selectivity for O_2, high carrier-oxygen binding constant
Advantages	High selectivity High diffusivity of the permeant molecule	High selectivity
Disadvantages	Loss of membrane solvent and carrier Low carrier concentration Carrier inactivation due to oxidation	Inactivation of the carrier after fixation in the solid state Non-uniformity in chemical reactivity of the fixed carrier Defect formation in the solid membrane Low diffusivity of the permeant molecule

2.1.3.1 Literature review of facilitated transport mechanism

Ward's [7] work provided a general understanding of facilitated transport. He carried out a mathematical and experimental investigation of facilitated transport. Nitrous oxide/ferrous transport was modeled as a basic facilitated transport reaction scheme. A mathematical model was developed for steady state permeation.

Donaldson and Quinn [8] also studied facilitated transport in liquid membranes for carbon dioxide separation. The model was developed for determining diffusional and kinetic parameters, but the derivation of the model equations was not clearly explained. Their work was used in later works on CO_2-amine systems for CO_2 capture.

Smith et al. [9] published a review on facilitated transport and provided a comprehensive summary of the research on facilitated membrane at that time. The

review covered facilitated transport of oxygen, carbon dioxide, and nitric oxide. They also provided a comprehensive documentation of the governing equations and the formulation of facilitation factor. Two years later, Smith and Quinn [10] also studied the facilitation factors in nitric oxide-ferrous ion facilitated transport systems with comparable results to the other studies and a CO_2-MEA system that had more complex chemistry. Meldon et al. [11] developed a model based on the standard reaction mechanism, and the permeation across the membrane was studied with an emphasis on the permeation time lag.

Matsuyama et al. [12] prepared poly(acrylic acid) / poly(vinyl alcohol) membrane for the facilitated transport of carbon dioxide. They introduced an ion-exchange membrane and used the monoprotonated ethylenediamine as the carrier of carbon dioxide. The highly swollen membrane by the aqueous solution had much higher CO_2/N_2 selectivity and CO_2 permeability than the Nafion membrane due to its higher ion-exchange capacity and solvent content. When the carbon dioxide partial pressure in the feed gas was 0.061 atm, a selectivity of more than 1900 was obtained. Teramoto et al. [13] studied the facilitated transport of CO_2 based on the amines MEA and DEA through supported liquid membranes. They found that the DEA system performed slightly better than the MEA system. A set of algebraic equations were used to solve the facilitation factor, and the mathematical model matched reasonably well with the experimental data.

Kavvali and Sirkar [14] used glycerol carbonate as a new physical solvent for carbon dioxide separation from CO_2/N_2 mixtures. The CO_2-selective behavior of the glycerol carbonate was investigated in an immobilized liquid membrane. They reported that the pure glycerol carbonate yielded a CO_2/N_2 selectivity of about 80-130 at various

CO_2 partial pressures. The selectivity was not affected by the humidity in feed and sweep streams. The CO_2 permeability across the membranes was about 100 barrer when the membranes were exposed to dry feed gas conditions. However, when the feed streams were humidified the permeability was increased to about 350 barrer. In addition, CO_2 facilitation at low CO_2 partial pressures was significantly increased by adding small amounts of facilitating carriers such as poly(amidoamine) dendrimer and sodium glycinate.

In case of facilitated oxygen transport, much of recent interest has been encouraged by the study of Scholander [15] on biological systems. He demonstrated that hemoglobin could accelerate the transport of oxygen in a liquid membrane with oxygen carriers. An eightfold increase in oxygen flux was obtained by using an aqueous solution of hemoglobin to replace pure water. The oxygen/nitrogen selectivity was about 14. However, hemoglobin was highly unstable in aqueous solutions outside of the body.

Bassett and Schultz [16] used synthetic oxygen carriers which were bis(histidine)cobalt(II) as a complexing agent in an aqueous medium. The best results obtained were an approximate doubling of the oxygen flux compared to water and the selectivity was 3.5. Even though it was a successful demonstration of facilitated oxygen transport, the carrier has two limitations. (1) even a saturated solution of the carrier shows only a limited increase in oxygen flux because it is not very soluble in the solvents. (2) it was quickly oxidized irreversibly, which makes it useless for facilitated oxygen transport. Therefore, much improvement is needed before it can become a useful process even though the concept of facilitated transport of oxygen has been demonstrated.

Johnson et al. [17] studied facilitated transport membranes for the production of oxygen-enriched air using membranes consisting of a transition-metal complex (Co(3-MeOsaltmen)) dissolved in a suitable solvent (γ-butyrolactone) and immobilized within the pores of a microporous membrane. An oxygen/nitrogen selectivity of over 20 was reported. In permeate stream, the oxygen purity was in the range of 80-90 mole% at 1 atm feed and a low pressure permeate. However, the oxygen permeability was about $26\times10^{-9} cm^3(STP)\cdot cm/cm^2\cdot s\cdot cmHg$, which was only about one-half that of silicone rubber. The lifetime of membrane was measured in weeks.

Nishide et al. [18] studied fixed cobalt porphyrin complex carriers over the last 15 years. They found that sorption and desorption of oxygen to and from the fixed carrier complexes in the membranes are very rapid and reversible. The oxygen permeability was enhanced by decreasing the feed stream pressure, and the oxygen transport was analyzed by dual mode transport. The selectivity of oxygen and nitrogen was more than 10.

2.1.4 Free-volume theory

Several theories had been proposed to describe the diffusion behavior, and Fujita proposed the free-volume theory. [19] Later, Vrentas and colleagues developed the theory to correlate accurately with the self-diffusion and binary mutual-diffusion coefficients at various temperatures and over a wide concentration range. [20] For the self-diffusion coefficient, it has been shown that the predictions of the free-volume theory are good for temperatures above the glass transition temperature of the polymer. [21] However, some difficulties may be encountered for systems at temperatures below

the pure polymer glass transition temperature. [22, 23] These difficulties are caused by uncertainties in the nature of the temperature dependencies of the various expansion coefficients of the theory.

The first proposed free-volume was for liquid media. However, in case of solid media, the state of the material has an influence on the gas permeability whether a polymer is in the glassy or rubbery state. The different permeability is due to the difference in thermal energy available for the mobility of the chain segment in the polymer. In glassy polymers, the mobility is limited, and the free-volume between polymer chains is frozen in the polymer matrix. Only a few segments of the chain have sufficient thermal energy for mobility. At high temperatures the polymer is in the rubbery state. The free-volume (i.e. some unoccupied space) exists between the polymer chains because they do not pack perfectly. As the temperature of the polymer decreases, the free volume also decreases. Above the glass transition, however, the mobility is increased and the "frozen" microvoids disappear inside the structure when the polymer is at the rubbery state. [4, 5]

The total polymer volume is viewed to consist of (1) the volume occupied by the molecular chain, (2) the interstitial free-volume, and (3) the hole free-volume. Generally, the empty space is considered as the free volume. The interstitial free-volume is small and uniformly distributed within the polymer structure, and the hole free-volume can randomly migrate through the polymer matrix. The approach of the hole free-volume is useful for describing transport of gas molecules through polymer matrix. The basic concept in the free-volume theory is that a molecule can diffuse from one place to another place if there is sufficient empty space or free-volume. If the size of the penetrant is increased, the amount of free-volume needed must be increased. In the case

of non-interacting systems, e.g. polymer with inert gas such as helium, hydrogen, oxygen, nitrogen or argon, the penetrant has no or little influence on the free-volume. Therefore, the free-volume is influenced mainly by temperature. [5]

2.1.5 Effect of temperature and pressure on permeability

The gas permeability and selectivity of polymer membranes are affected by the temperature. When the operating temperature is increased, the permeability is increased but the selectivity of membranes is often decreased due to the increased polymeric chain mobility. [24] The diffusion of gases through polymer membranes is an activated process and can be described using Arrhenius type equations. The relationships for D, S, and P as a function of temperature can be expressed as: [25]

$$D = D_{\circ} \exp\left(-E_d / RT\right) \tag{2.7}$$

$$S = S_{\circ} \exp\left(-\Delta H_s / RT\right) \tag{2.8}$$

$$P = P_{\circ} \exp\left(-E_p / RT\right) \tag{2.9}$$

where constant $D_{\circ}$, $S_{\circ}$ and $P_{\circ}$ are the pre-exponential factors. E_d is the activation energy of diffusion, ΔH_s is the heat of sorption, and $E_p (= E_d + \Delta H_s)$ is the activation energy of permeation. Theses equations indicate strong temperature dependencies of permeability and selectivity. However, for different gases temperature will influence the various transport parameters differently.

Plasticization can occur at a high pressure of gas in both glassy and rubber polymers. The permeability is increased with the feed pressure when the gas acts as a plasticizer for the polymer. The permeability coefficient would not change with the feed pressure for non-interacting gases such as N_2 and He. The permeability coefficient is

found to be pressure or concentration dependent in an exponential or linear fashion for larger and condensable gases such as CO_2. [26] The effect of the feed pressure can be more complicated due to the dual-sorption effect in glassy polymers; In this case, depending on the type of the polymer and penetrant, the feed pressure can cause the permeability to increase or decrease at a high pressure because of the competing effect of the penetrant in the polymer.

2.2 Carbon dioxide/nitrogen separation

The supported liquid membrane (SLMs) containing a mobile carrier in membrane pores have been studied due to their high selectivity toward carbon dioxide for the separation of carbon dioxide. However, it is still difficult to apply the liquid membrane for practical use because the carrier is unstable. [3, 27] The gel-type swollen membrane, an intermediate between liquid and solid phase, can be made by swelling a polymer film in a solvent. The solvent-swollen membrane can be used as a gas separation membrane if the solvent used to swell the polymer film is a good physical solvent for the gas of interest.

Ito et al. [28] used a wet chitosan membrane to permeate N_2, CO_2, and CH_4. The influence of the membrane preparation and operating conditions on the separation performance of the wet chitosan membrane was studied. In their study, carbon dioxide preferentially permeated through the swollen chitosan membrane with a permeability of $2.5\times10^{-8} cm^3(STP)cm/(s\cdot cm^2\cdot cmHg)$ and a CO_2/N_2 separation factor of 70 at room temperature.

Matsuyama et al. [29] prepared an ion exchange membrane by grafting acrylic acid onto a microporous polypropylene by the plasma-grafted polymerization technique. They studied the facilitated transport of CO_2 through the grafted membrane carried out by using various diamines, diethylenetriamine and triethyleneteramine as the carrier. The grafted acrylic acid membrane containing ethylenediamine as the carrier showed the highest selectivity of CO_2 over N_2.

Park et al. [27] studied a water-swollen hydrogel membrane for gas separation by dip-coating a poly (vinyl alcohol) solution containing glutaraldehyde as a crosslinking agent on an asymmetric porous polyetherimide support. The study was successfully applied to the carbon dioxide separation over a long period. The gas permeation behavior through the water-swollen hydrogel membranes was discussed. The behavior of gas permeation through the membrane was parallel to the swelling behavior of the membrane in water. Through the water-swollen hydrogel membranes the permeance of carbon dioxide was $10^5 cm^3/\left(cm^2 \cdot s \cdot cmHg\right)$ and a CO_2/N_2 separation factor was about 80 at room temperature. The influence of the additive and catalyst on the permeation of gases through the membranes was also studied.

Yeom et al. [30] investigated the permeation of mixed CO_2/N_2 gases through poly(dimethylsiloxane) (PDMS) at various operating conditions. They evaluated the permeation and separation behavior in terms of permeability, diffusion and solubility coefficients. The effects of operating temperature and feed pressure on the permeation were studied. The solubility coefficients of CO_2 and N_2 were found to be affected by feed pressure and temperature. Increasing feed pressure increases CO_2 solubility coefficient and decreases N_2 solubility coefficient, and on the other hand, increasing temperature favors only N_2 sorption.

Kim et al. [3] prepared water-swollen membrane for gas permeation using Na-alginate and poly (vinyl alcohol) blend membranes. They investigated the influences of water content and crystallinity of the membranes on the gas permeation performance. Using the water-swollen membranes, the permeation rates of nitrogen and carbon dioxide were in the range of $(0.4-7.6)\times10^{-7}$ to $(3.7-8.5)\times10^{-6}\ cm^2(STP)\cdot cm/(cm^2\cdot s\cdot cmHg)$, which were 10,000 times higher than those of dry-state membranes. They found that the gas permeance of the water-swollen membranes increased with increasing the Na-alginate content in the membrane and the gas permeation rates of the membranes increased with increasing the water content in the membrane.

2.3 Oxygen/nitrogen separation

Oxygen and nitrogen separation is one of the main applications as commodity chemicals. Generally, they are produced from air by pressure swing adsorption or cryogenic distillation. Since these processes are highly energy intensive, the number of current applications is limited and a less costly process is desirable. As a possible alternative, gas separation membranes have been considered for the production of oxygen and nitrogen. However, the production of nitrogen from air using membranes is limited to moderate purities and the production of oxygen-enriched air is only at a relatively small scale. Extensive effort has been made in the last 30 years to overcome low permeability and selectivity of conventional membranes.

Lehermeier et al. [31] examined the permeation of nitrogen, oxygen, carbon dioxide and methane in amorphous films of poly(lactic acid). Comparing with other

commodity plastics, the properties of the membranes closely resembles that of polystyrene membranes. At $30^{\circ}C$, nitrogen and oxygen permeability were $1.3\times10^{-10}cm^3(STP)\cdot cm/(cm^2\cdot s\cdot cmHg)$ and $3.3\times10^{-10}cm^3(STP)\cdot cm/(cm^2\cdot s\cdot cmHg)$, respectively. In addition, the permeability of carbon dioxide and methane was $1.2\times10^{-10}cm^3(STP)\cdot cm/(cm^2\cdot s\cdot cmHg)$ and $1.0\times10^{-10}cm^3(STP)\cdot cm/(cm^2\cdot s\cdot cmHg)$, respectively. The separation factor of carbon dioxide and methane was measured at different temperatures (0-50$^{\circ}C$).

Wang et al. [32] prepared ethylene-diamine-teraacetic acid disodium salt (EDTA)-methyl metacrylate butyl acrylate copolymer by radical polymerization in an aqueous solution. EDTA, which chelated cobalt ions (Co^{2+}) and was at the chain end of compolymer, was used as an oxyphilic carrier. The prepared chelated compolymer membranes with different cobalt contents showed a good oxygen permeability of $10\times10^{-9}cm^3(STP)\cdot cm/(cm^2\cdot s\cdot cmHg)$ and an oxygen/nitrogen selectivity of 10. The separation factor was increased with an increase in Co^{2+} contents in the membrane. The relationship between the oxygen or nitrogen permeability and temperature follows the Arrhenius equation, and the diffusion activation energies of oxygen and nitrogen were estimated to be 7.4-11.4 and $12\,kcal/mol$, respectively.

Morisato and Pinnau [33] prepared a poly(4-methyl-2-pentyne) film, which is an amorphous and glassy polymer, for oxygen and nitrogen permeation. Oxygen and nitrogen permeabilities of 2700×10^{-10} and $1330\times10^{-10}cm^3(STP)\cdot cm/(cm^2\cdot s\cdot cmHg)$, were observed at $25^{\circ}C$, respectively. It was found that the high gas permeabilities were related with the very high free volume, and probably the interconnectivity of the free volume elements as well.

2.4 Background of silk sericin

Sericin, the second major *B. mori* silk protein, has excellent properties, antioxidative, antibacterial, UV resistant and moisture-absorbing and -desorbing properties. It can be applied to many fields such as cosmetic, medical and polymer materials. Silk obtained from silkworm *Bombyx mori* is a natural protein which is made of sericin and fibroin proteins. Sericin generally constitutes 25% of silk protein. It glues the fibroin fiber with successive sticky layers in the formation of a cocoon. From the silkworm *Bombyx mori,* there are two kinds of proteins in silk filament: sericin (the outer coating) and fibrioin (the inner core), which are both natural macromolecular biopolymers, as shown in Figure 2-4. [34-36]

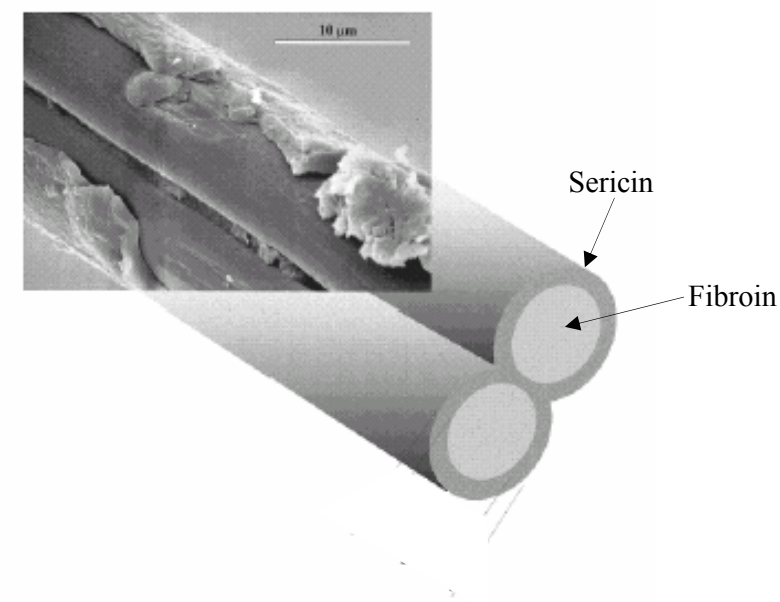

Figure 2-4 Structure of Silk [34]

Sericin is removed by degumming process in the silk industry and the waste water is mostly discarded from silk processing. Sericin is a water soluble glue protein, unlike silk fibroin which is an oriented fiber protein. During raw silk production at the reeling

mill, most of the sericin must be removed. The fresh weight of the cocoon production is about 1 million tons worldwide and it is equivalent to 400,000 tons of dry cocoon. About 50,000 tons of sericin is produced from the process of the raw silk production. It represents significant economic and social benefit if this sericin protein is recovered and recycled. [37]

During the degumming treatments in boiling water or an alkaline solution, sericin is easily isolated from the inner core, fibroin, and degraded into sericin peptides, ranging widely from about 10 to over 300 kDa in molecular weight, depending on operating temperature, pH, and the processing time. [38] Peptide is a compound that is made up of two or more amino acids joined by covalent bonds which arise by elimination of H_2O from the carboxyl group of one amino acid and the amino group of the other amino acid. The general structures of protein and polypeptides are shown in Figures 2-5 and 2-6, respectively. [39, 40] The structures of amino acids of sericin are shown in Table 2-3. [40] The sericin protein has 18 amino acids which mostly constitute serine and aspartic acid (approximately 33.4% and 16.7% of sericin, respectively). The sericin peptides having a lower molecular weight of less than 60 kDa, commonly less than 5 kDa, are soluble in cold water and can be recovered at early stages of raw silk production. This sericin can be characterized by excellent moisture absorption and release, and biological activities such as antioxidation, tyrosinase activity inhibition, and pharmacological functions (e.g., anticoagulations, anticancer activities, cyroprotection and promotion of digestion). The rest portion, a higher range of molecular weight from 60 to over 300 kDa, is poorly soluble in cold water but soluble in boiling water and can be obtained at the later stages of silk processing or silk degumming. Due to its properties, sericin is particularly useful for improving polymer materials such as

polyesters, polyamide, polyolefin, and polyacrylonitrile. Moreover, it can also be applied to degradable biomaterials, biomedical materials, functional bio-membrane materials and functional fibers. [37, 41]

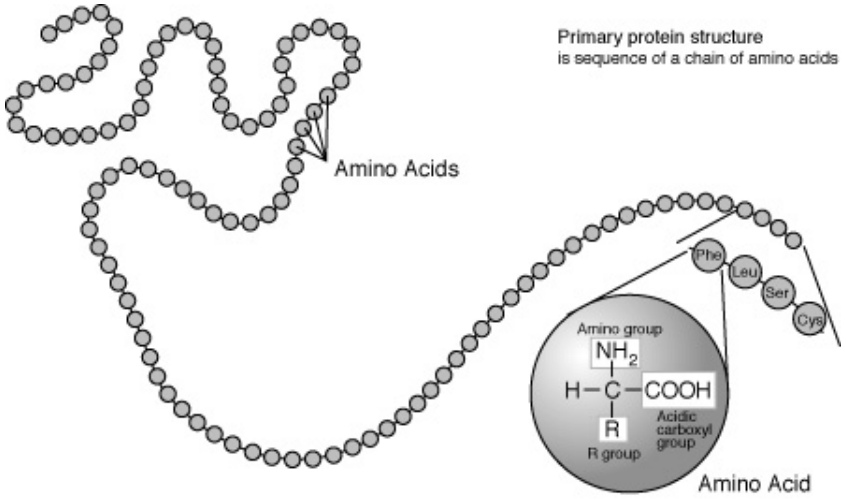

Figure 2-5 Structure of primary protein [39]

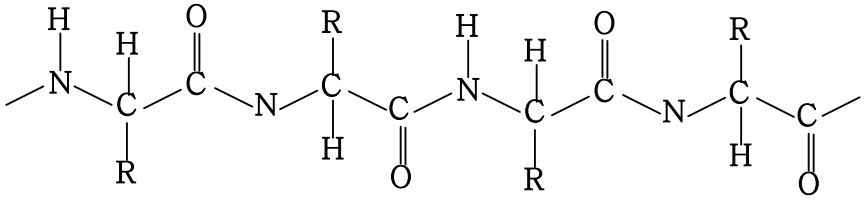

Figure 2-6 Structure of polypeptide [40]

Table 2-3 Structures of amino acids of silk sericin [40]

Amino acid	Structure	Amino acid	Structure
Aspartic acid	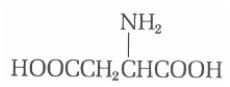	Methionine	
Threonine	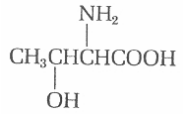	Isoleucine	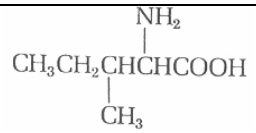
Serine	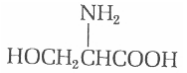	Leucine	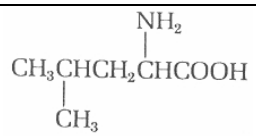
Glutamic acid		Tyrosine	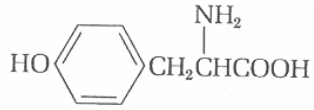
Proline	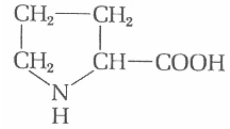	Phylalanine	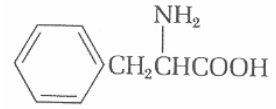
Glycine	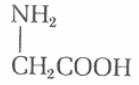	Lysine	
Alanine		Histidine	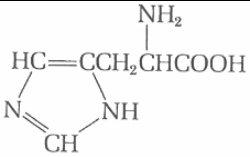
Cysteine	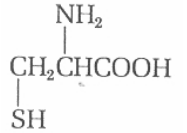	Arginine	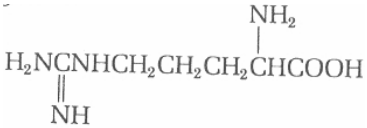
Valine	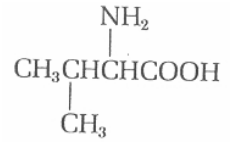	Tryptophane	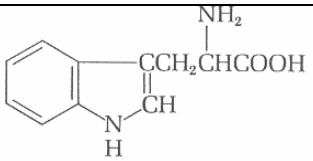

2.4.1 Extraction methods

Removal of the sericin from silk fibroin is accomplished by a process called "degumming", usually by one of the following methods: (1) extraction with water at a high temperature, (2) extraction with water at a high temperature and under pressure, (3) extraction with a soap solution, (4) extraction with a synthetic detergent, (5) extraction with an acid, and (6) removal by enzymes. [42, 43] The degumming process is generally used to remove the silk sericin from the fibers in the silk industry. [43]

(1) Extraction with water treatment

This is the easiest extraction method to get sericin solution and it is also used for this study. The cocoon shells of *Bombyx Mori* were cut into pieces (about $1cm^2$) or so and thoroughly washed with water. The cocoon shells were then boiled with water at 95-100$^\circ C$ for different periods of time. To remove fibroin, it is filtered by using filtration methods such as non-woven fabrics and glass microfiber filter. [44-47]

(2) Extraction with water under pressure at 120$^\circ C$

Sericin can not be dissolved in room temperature water, but it is highly susceptible to dissolution in boiling water. For this reason, there is a risk that fibroin may be damaged when the treatment is sufficiently long. In the silk industry, autoclaves (commonly at 120$^\circ C$ and 2 atmospheres for 1-2 hr) are normally used to treat the fiber. [41, 48-53] However, incomplete degumming may occur. That is why sometimes soap or synthetic detergent is added to improve the degumming effect. This process, therefore, is very difficult to control and it is not widely used in the silk industry nowadays.

(3) Extraction with soap solutions

Marseilles soap is an outstanding soap for sericin extraction. This process, for example, can be carried out using 10-20 g/l soap at 92-98$^{\circ}C$ for 2-4 hours at pH 10.2-10.5. Generally, alkali causes hydrolysis of the polypeptide chains in the fibers. In addition, alkali hydrolysis can attack the end of a peptide chain easily. [29] Due to the sensitive nature of fibroin itself and the chemical similarity of fibroin and sericin, this process tends to attack both sericin and fibroin at high temperatures. Moreover, the most important requirement for this process is that soft water should be used to avoid the formation of calcium soap. [49, 54] Nowadays, soap solution is replaced by synthetic detergents because they have some advantages over soap such as reducing the extraction time and damage of the fiber. [29]

(4) Extraction with synthetic detergents

Synthetic detergent can be used to minimize the fiber damage and reduce the time of treatment (e.g., 30-40 min at 98$^{\circ}C$) compared with soap. Non-ionic synthetic detergent can reduce the impact on the tensile strength of the fiber in the extraction process of sericin. Normally, efficient degumming can be achieved using 2.5 g/l non-ionic synthetic detergent at pH 11.5 for 30 minutes. A problem of this process, however, is the still relatively high temperature (e.g., at 98$^{\circ}C$) and high pH (e.g., at pH 11.5). Therefore, the operating temperature, time of treatment and amount of detergent should be properly controlled to prevent damage to the fibroin. [49, 54-57]

(5) Extraction with acids

Some acids (such as sulphuric, hydrochloric, tartaric and citric acids) can be used as degumming agents. Because the alkaline solutions are safer to fibroin degradation than acid solutions, this process has not received much attention in the silk industry. Strong mineral acids (e.g., sulphuric and hydrochloric acids) cannot be used to achieve complete degumming without damaging fibroin. [55]

(6) Removal with enzymes

Enzymes appear in living cells, catalyzing a specific chemical reaction as bio-catalysts. They can be used at atmospheric pressure and in mild conditions (e.g., at 40 $^{\circ}C$, pH 8.0). Different enzymes may cause hydrolysis, reduction, oxidation, coagulation and decomposition reactions. Hydrolytic enzymes are commonly used in the textile industry: e.g., cellulase, trypsin and papain. [58]

Among the various processes discussed above, soaps or synthetic detergents are used for degumming on an industrial scale. These methods are good for silk processing, but it is difficult to get high quality sericin. Water treatment at over 90 $^{\circ}C$ appears to be one of the best ways to extract the sericin with molecular weights 20-200 kDa. Using the water treatment method, there is no need to remove the chemicals and treat the waste water generated. Due to its economic advantage, sericin extraction with water is widely used nowadays. The yields of silk sericin extracted using different methods are listed in Table 2-4.

Table 2-4 Yield of sericin extracted with different methods

Extraction methods	Yield	Reference
Water (at 95-100 $^{\circ}C$)	14.3%	[44]
	22.5%	[59]
Acid (6N HCl at 110 $^{\circ}C$)	23.18%	[60]
Enzyme (Protease)	19%	[38]

2.4.2 Characteristics of silk sericin

The amino acids in sericin consist of 18 amino acids, among which the polar amino acids with hydroxyl and amino groups such as aspartic acid, serine and lysine account for 72%, as shown in Table 2-5. [41] The amino acid classification for silk sericin is shown in Table 2-6. [61] The first group is polar uncharged amino acids that possess oxygen, sulphur and/or nitrogen in the side chains. The polar nature of the side chains means that these amino acids readily interact with water, i.e. they are hydrophilic. The second group, polar amino acids with positively charged side chains, is not only polar but can also carry a positive charge and are therefore also hydrophilic. Another group is polar amino acids with negatively charged side chains that there are only two amino acids, Asparate (Aspartic acid) and Glutamate (Glutamic acid), with negatively charged (i.e. acidic) side chains. Figure 2-7 shows the hypothetical intermolecular interactions between silk fibroin and silk sericin. If silk fibroin and silk sericin are considered as the primary structure, each protein has a repeated amino acid sequence that is capable of forming the β-sheet structure. The silk sericin has the repeat sequence of GSVSSTGSSNTDSST, and the silk fibroin has the sequence of $[GAGAGS]_n$, where G, A, S, T, V, N and D denote glycine, alanine, serine, threonine,

valine, asparagines and aspartic acid, respectively. Sericin has the hydroxyl groups regularly on one side of the peptide backbone (see the arrow). There are hydrogen bonds (dotted lines) formed between the oxygen of the C=O in the silk fibroin and the OH and NH hydrogens in silk sericin if silk fibroin and silk sericin approach each other. [54, 62]

Table 2-5 Amino acid composition of water-soluble sericin (mol%) [41]

Amino acid	**Content**	**Amino acid**	**Content**
Aspartic acid	20.55	Methionine	0.00
Threonine	7.96	Isoleucine	0.88
Serine	25.28	Leucine	1.36
Glutamic acid	7.90	Tyrosine	4.47
Proline	0.00	Phylalanine	0.91
Glycine	10.51	Lysine	4.68
Alanine	3.97	Histidine	1.75
Cysteine	0.72	Arginine	5.26
Valine	3.79	Tryptophane	0.00

Table 2-6 Classification for amino acid of silk sericin [61]

Classification	Amino acid
Polar uncharged amino acid	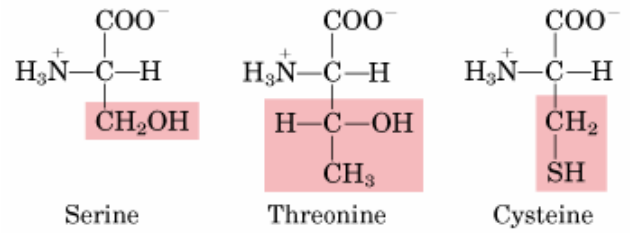 Serine Threonine Cysteine
Polar amino acids with positively charged side chains	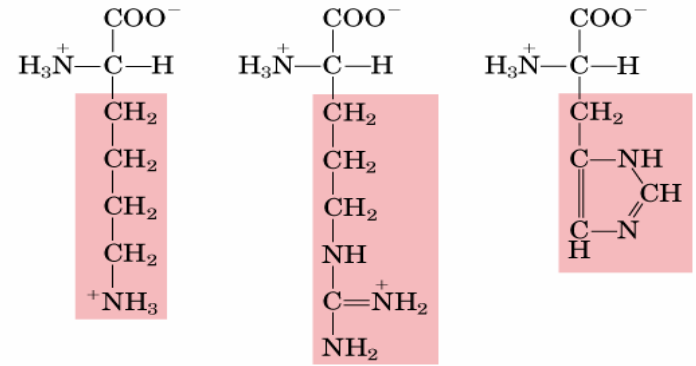 Lysine Arginine Histidine
Polar amino acids with negatively charged side chains	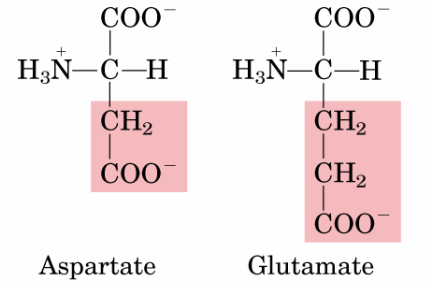 Aspartate Glutamate

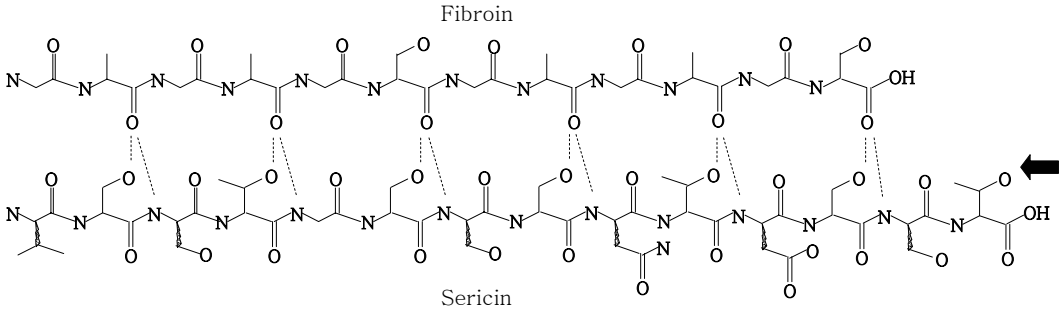

Figure 2-7 Schematic representation of the intermolecular hydrogen bonding at the boundary of silk fibroin and silk sericin [54]

The secondary structure of silk sericin is various due to its preparation conditions, but it mostly constitutes of random coil structure and little amount of β-sheet structure. Generally, as sericin is close to fibroin, the amount of β-sheet structure is increased. Extracted sericin solution is turned to gel state after certain period of time due to increased amount of β-sheet structure. However, it can be returned to sol state upon heating. The sol state is a colloidal suspension that can be gelled to form a solid. The sol-gel state change involves the transition of a system from a liquid (the colloidal "sol") into a solid (the "gel") phase. This characteristic of sol-gel transition is different from fibroin. Alcohol generally changes fibroin to β-sheet structure, but sericin can not be perfectly changed. Lee [63] studied whether alcohol, acetone and water at $110^{\circ}C$ can affect the structure of sericin. After being treated with those solutions, some of random coil structure is found to have changed to β-sheet structure.

Kweon et al. [45] found that the gelation time of silk sericin decreased with an increase in poloxamer concentration and temperature, and the structure change of silk sericin from random coil to β-sheet structure was accelerated by adding poloxamer because the hydrophilic parts of poloxamer absorbed the water surrounding the sericin molecules. Gelation of silk sericin is thermo-reversible by itself, but in the presence of poloxamer the gelation became irreversible with temperature change. Interestingly, the gelation of silk fibroin in the presence of poloxamer is reversible, whereas that of silk fibroin is irreversible by itself. Because of the differences in chemical composition between silk sericin and silk fibroin, sol-gel transition of silk sericin in the presence of poloxamer was completely different from that of silk fibroin.

It is generally acknowledged that thermal treatment of sericin especially in the presence of organic solvents or water affect the sericin structural changes from random coil to β-sheet. Sericin transformed into an aggregated state by water and organic solvent. Aggregated strands contain strong hydrogen bonds. The strong interchain interaction might result from the abundance of polar side chains such as hydroxyl and carboxyl groups, which can form interchain hydrogen bonds with other polar side chains or amide groups in peptide backbone. Sericin can be transformed into a β-sheet structure having strong intermolecular hydrogen bonds. [64] Teramoto et al [64] found that using ethanol for β-sheet formation of silk proteins is more effective than using methanol. In addition, using ethanol is less toxic than methanol, which is advantageous for sericin's application as a biomaterial.

2.4.3 Literature review of sericin / PVA blend

The structure and physical properties of silk sericin have been studied by many researchers as mentioned before. Some studies have focused on the extraction methods applied to the waste solution from the textile manufacturing process. Broader uses of sericin are expected for efficient utilization of sericin. On the other hand, PVA is widely employed in fiber, film, and adhesive production, and is also used in paper making. Even though it has a high melting point and viscosity for molding of PVA, it is a promising polymeric material due to its high tenacity and modulus.

Miyake et al. [65] developed an injection molding plastic blend of PVA and sericin, and studied its physical properties and structure with various content rates of sericin. In their study, the stress and strain were increased at a sericin content rate of 2 wt%.

However, the stress and strain values were decreased at 5 wt% sericin, and increased again above 10 wt% sericin. The blended material at a sericin content of below 20 wt% has random coil structure. On the other hand, at a sericin content of 30 wt%, both structures, random coil and β-sheet structures, are present.

Chapter 3
Experimental methods

The main objective of the study was to prepare suitable water-swollen sericin / polyvinyl alcohol (PVA) membranes for gas separation. Water-swollen membranes are expected to be more effective than dry membranes in terms of selectivity and permeability. The extraction of sericin from cocoons was carried out and the molecular weight of sericin was evaluated. Due to the hydrophilicity of sericin and PVA, water-swollen membranes were easily prepared by using crosslinking agent. Different sericin / PVA compositions in the blend membranes were studied. In addition, water swelling and water vapor sorption/desorption characteristics of the membranes were studied.

3.1 Materials

Sericin was extracted from cocoons, *Bombyx mori*., using hot water. Polyvinyl alcohol powder (Mw ~133,000, 99 mole% hydrolyzed) was purchased from Polysciences. Glutaraldehyde solution ($C_5H_8O_2$) (25 wt% aqueous solution) was purchased from Sigma. Deionized water was supplied by the Department of Chemical Engineering.

3.2 Sericin extraction and characterization

3.2.1 Extraction of silk sericin

In this study, water extraction was used to obtain sericin from silkworm cocoon. The cocoon shells of *Bombyx Mori* were cut into pieces (about $1cm^2$) and washed with deionized water with air flotation. After removal of impurities by filtration, the washed cocoon shells were dried. The dried cocoon shells (1g) were immersed in water (50g of total weight) to initiate sericin extraction. The samples were kept in a glass bottle placed in a water bath. After extraction at a given temperature (25-95$^\circ C$) for a given period of time (0.1-9 hr), the undissolved cocoons were filtered by non-woven fabrics. The solution was dried and the sericin sample powder was yellowish in color. The yield of sericin and the concentration of sericin solution were calculated.

$$\text{Yield of sericin [\%]} = \frac{W_d}{W_c} \times 100 \tag{3.1}$$

$$\text{Concentration of sericin solution [\%]} = \frac{W_d}{W_s} \times 100 \tag{3.2}$$

where, W_d and W_s are the weight of dried silk sericin and the weight of silk sericin solution after the filtration, respectively. W_c is the weight of dried cocoon shells.

3.2.2 Sodium dodecyl sulfate-polyacrylamide gel electrophoresis test

The sericin solution after filtration was mixed with sodium dodecyl sulfate polyacrylamide gel electrophoresis (SDS-PAGE) sample buffer (0.1 M Tris-HCl (BioShop, CA) of pH 6.8, 4% SDS (EM Science, Germany), 12% 2-mercaptoethanol (Sigma, Germany), 20% glycerol (Fischer Biotech)) and boiled for 5 min. The sample

was adjusted to pH 6.8 with dilute HCl (Fischer Scientific) solution immediately before electrophoresis. The range of molecular weight of sericin was determined by SDS-PAGE according to the method of Laemmli. [66] Samples (20 μL) were electrophoresed in running buffer (1% SDS; 192 mM glycine (BioShop, CA); 25 mM Tris-base (BioShop, CA); pH 8.3) on a 10% resolving gel (10% acrylamide/bisacrylaminde (BioBasic, CA), 375 mM Tris-HCl, 0.1% SDS, pH 8.8) at 100-130V for 1.5h using a Mini-PROTEAN II vertical cell system (Bio-Rad, CA). The molecular weights of the sample were estimated using a molecular weight marker (Precision Protein Standards, range 11-170 kDa; Bio-Rad, CA) The gels were stained with Coomassie Brilliant Blue R 250 dye (BDH, CA) and destained with 45% methanol, 10 acetic acid (BioShop, CA) to visualize the proteins.

3.2.3 UV/vis spectroscopy

Silk sericin solution obtained from the extraction was examined by using UV/vis spectrophotometer (UV mini 1240, SHIMADZU).

3.3 Membrane preparation

3.3.1 Pure PVA membranes

1. 10 wt% of PVA solution was prepared with dry PVA and deionized water. The pre-weighed dry PVA was dissolved in water and stirred at $90^{\circ}C$ for 6 hrs on a tightly capped glass container.

2. When the solution was transparent, it was filtered under vacuum with a porous glass filter. After the solution was cooled down, small amount of glutaraldehyde (as a crosslinking agent) was added into the solution and stirred for 3 hours.

3. The membrane was cast onto a glass plate using a glass rod. The casting thickness was controlled to be $268\ \mu m$ using copper wires.

4. The membrane was dried in a clean fume hood at room temperature for at least 1 day.

5. After drying, the membrane was heat treated at $120^{\circ}C$ for 1 hour in order to crosslink PVA.

3.3.2 Sericin / PVA membranes

1. Sericin and PVA solutions were prepared first, then they were mixed in various ratios and stirred for one day. Glutaraldehyde was added into the solution and stirred for 3 hours. The mass ratio of glutaraldehyde to sericin and PVA solution was 1 to 100.

2. The membrane was cast on a glass plate, as described before.

3. Once the membrane was dried, it was heat treated at $120^{\circ}C$ for 1 hour to crosslink the membrane.

3.4 Permeation experiments

3.4.1 Experimental set-up

The schematic diagram of experimental set-up for gas permeation is shown in Figure 3-1. The membrane was first swollen with deionized water. Then, the membrane was mounted in the membrane cell (permeation area $15.2\,cm^2$). Feed gas at a low pressure (<5 psi) was flushed to remove the air inside the permeation cell. The feed pressure was gradually adjusted to an operating pressure (in the range of 30-60 psi) until steady-state was reached, which could be assumed when the flow rate no longer changed with time. The permeate flow rates were measured using a bubble flow meter. The steady-state permeation was reached in 3 hours. All measurements were tested at room temperature and repeated at least twice.

The feed gas, pure carbon dioxide oxygen and nitrogen, was supplied by Praxair and the feed pressure was monitored using a Cole-Palmer pressure gauge. The feed gas was saturated with water before entering the permeation cell in order to keep the membrane continuously swollen during the experiments.

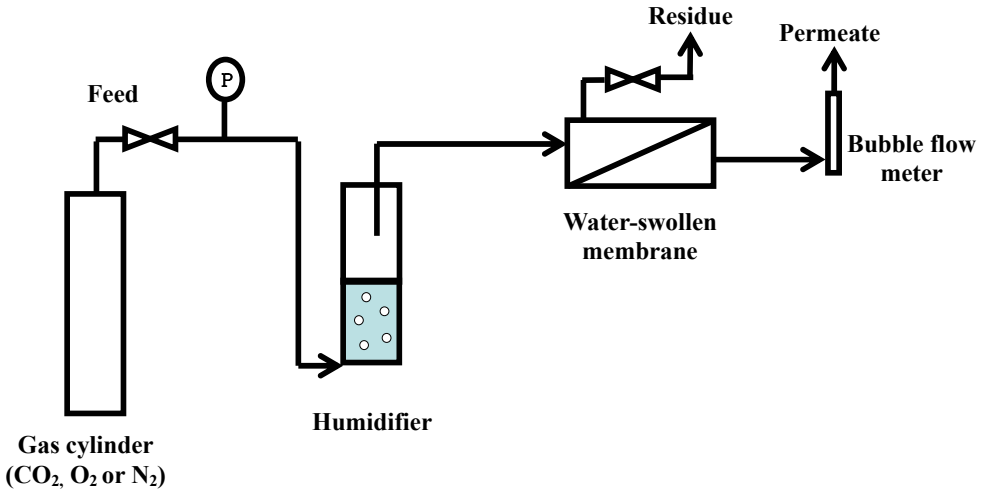

Figure 3-1 Schematic diagram of experimental set-up for permeation tests

3.5 Characterization of the membrane properties

Permeability and selectivity

From the experiments the permeability and selectivity can be evaluated. The permeability P_i can be calculated from:

$$P_i = \frac{Fl}{A\Delta p} \tag{3.3}$$

where P_i is the permeability of the gas (conventionally expressed in Barrer, 1 Barrer = $10^{-10} cm^3(STP)cm/(cm^2 \cdot s \cdot cmHg)$), F is the permeation rate through the membrane ($cm^3(STP)/s$), and l and A are the thickness of the membrane (cm) and the area (cm^2) of membrane for permeation, respectively. Δp is the pressure different across the membrane.

Selectivity is expressed by the ratio of the individual gas permeabilities. It is a measure of the ability of a membrane to separate two gases. Based on permeabilities of pure gases "i" and "j", the ideal selectivity can be calculated:

$$\alpha_{ij} = \frac{P_i}{P_j} \tag{3.4}$$

A sample calculation of the permeability and selectivity can be found in Appendix A.

Swelling ratio

The swelling ratio of a membrane can be defined as water uptake per mass of dry membrane weight.

$$Swelling\ ratio = \frac{W_w - W_d}{W_d} \times 100 \tag{3.5}$$

where W_w and W_d are the weight of water-wet membrane and dry membrane, respectively.

The swelling ratio was determined as follows:

1. The membrane sample was washed and put into deionized water for 2 days to make sure that the membrane was fully saturated with water.
2. The wet membrane surface was blotted quickly with a clean tissue paper and the weight of the wet membrane (W_w) was measured.
3. After the weight was measured, the water-wet membrane was dried in a vacuum oven at $25^{\circ}C$.
4. The weight of the dry membrane (W_d) was measured, and then the swelling ratio was calculated using equation (3.5).

Because water sorption in the membrane was very quick, it was difficult to measure the water sorption rate using the above method. Therefore, water vapor sorption/desorption experiments were also conducted in order to evaluate the water diffusion in the membrane.

Water vapor sorption and desorption

In this experiment, the membrane samples were exposed to water vapor and the changes in the mass of the membrane with time were monitored using an analytical balance. Therefore, the mass gain due to sorption can be used to determine the diffusion coefficient of water in the membrane. Similarly, the mass loss due to desorption of water vapor was also performed. For the water vapor sorption test, a washed membrane

by deionized water was placed in vacuum oven at $25^{\circ}C$ to be dried. After dried, the membrane is exposed to the water vapor, 55% RH at $25^{\circ}C$. Then, the weight of membrane was measured in different time until the weight of membrane was not changed. Water vapor uptake in the membrane is represented by

$$\frac{M_t}{M_\infty} = \frac{W_{ts} - W_0}{W_\infty - W_0} \tag{3.6}$$

where W_{ts} is the weight of the membrane at time t, W_0 is the initial weight of the dry membrane, W_∞ is the weight of membrane at sorption equilibrium ($t = \infty$). M_t / M_∞ represents the fractional quantity of water sorbed in the membrane at time t.

Similarly, for the water vapor desorption test, a membrane was washed and fully swollen in deionized water. The swollen membrane surface was blotted as quickly as possible by clean tissue and it was exposed to the water vapor, 55% RH at $25^{\circ}C$, to be desorped to the air. Then, the weight of membrane was measured in different time until the weight of membrane was not reduced at all. For the desorption of water vapor from the membrane, the following equation can be used to represent the fractional quantity of water remaining in the membrane at time t:

$$\frac{M_t}{M_\infty} = \frac{W_{td} - W_0}{W_\infty - W_0} \tag{3.7}$$

where W_{td} is the weight of the membrane at time t.

From the M_t / M_∞ versus t data, if the diffusion follows Fick's law, the diffusion coefficient D can be calculated using the equation (3.8): [67]

$$\frac{M_t}{M_\infty} = 1 - \left(\frac{8}{\pi^2}\right)\sum_{n=0}^{\infty}\left\{\frac{1}{(2n+1)^2}\exp\left[\frac{-D(2n+1)^2\pi^2 t}{l^2}\right]\right\} \tag{3.8}$$

where l is the thickness of the membrane.

In the early stage of sorption and desorption, i.e. for small t values, the above equation can be approximated by a linear relation between M_t / M_∞ and $t^{1/2}$: [68, 69]

$$\frac{M_t}{M_\infty} = 4\left(\frac{Dt}{\pi l^2}\right)^{1/2} \tag{3.9}$$

Thus, the diffusivity coefficient can also be estimated from the slope of M_t / M_∞ vs $t^{1/2} / l$ plots.

Chapter 4

Results and discussion

As mentioned in chapter 1, separation of carbon dioxide from flue gas is important for greenhouse gas emission control. Moreover, oxygen enriched air is required in many applications. In this study, the property and performance of the sericin / PVA membranes for gas permeation were evaluated. The effects of sericin content in the membrane were studied. The water-swollen membranes were prepared using sericin and PVA as hydrophilic materials. The silk sericin extracted from cocoons at 95$^{\circ}C$ for 9 hours was used to blend with PVA to prepare blend membranes. However, it was too brittle to use as a membrane for gas permeation when the sericin content was more than 31 wt%. In addition, the effects of water in the membranes were studied by water swelling and water vapor sorption/desorption experiments, and diffusion coefficient could be determined from the experimental data.

4.1 Extraction of silk sericin

Figure 4-1 shows the yield of sericin obtained by extraction with water at a given temperature (25-95$^{\circ}C$) for a given period of time (0.1-9 hours). From the experimental data, the highest yield of sericin (22.8%) was obtained at 95$^{\circ}C$ for 9 hrs. Generally, cocoon shell has 25% of silk sericin [34-36], which means that most silk sericin was extracted (22.8%) from silkworm cocoons in this study. For a given period of extraction, the yield of sericin did not improve significantly when the temperature changed from 25 to 75$^{\circ}C$. However, increasing the temperature to 85-95$^{\circ}C$, the extraction became much more efficient. It can be thought that the lower molecular weight of sericin can be extracted at lower temperatures and the higher molecular weight sericin started to be dissolved in water at higher operating temperatures (85-95$^{\circ}C$). To quantatively study the yield of sericin at various operating temperatures and time, Equation (4.1) was proposed to correlate the sericin yield with extraction time at different temperatures:

$$\frac{Y_t}{Y_\infty} = 1 - \exp\left(-bt^n\right) \tag{4.1}$$

where Y_t is the yield of sericin at time t and Y_∞ is the total sericin content in the cocoon (which is assumed to be 25%). Parameters b and n are a function of temperature of extraction. Equation (4.1) can be rewritten as

$$-\ln\left(1 - \frac{Y_t}{Y_\infty}\right) = bt^n \tag{4.2}$$

or

$$\log\left[-\ln\left(1 - \frac{Y_t}{Y_\infty}\right)\right] = \log b + n\log t \tag{4.3}$$

From the equation (4.3), parameters b and n can be found by plotting

$\log[-\ln(1-Y_t/Y_\infty)]$ versus $\log t$, which shows a linear relation as shown in Figure 4-2. The parameters at different temperatures are shown in Table 4.1.

Table 4.1 Value of parameter b and n at different temperatures

Operating temperature [$^\circ C$]	Parameter b	Parameter n
25	7.32×10^{-2}	18.43×10^{-2}
50	7.73×10^{-2}	23.43×10^{-2}
75	11.14×10^{-2}	19.41×10^{-2}
85	7.92×10^{-2}	40.66×10^{-2}
95	12.08×10^{-2}	47.41×10^{-2}

It can be seen that both b and n tend to increase as the extraction temperature increases, except for an extraction temperature of $75^\circ C$. The reason for this is still unclear. It could be caused by the experimental error in thermostat setting as well as the variation in the cocoon samples. Further study is needed to clarify this. Nevertheless, it is shown that the sericin extraction rate can be described by the 2-parameter equation (Eqn 4.1).

4.2 Molecular weight

The silk sericin samples obtained by water extraction for 9 hours at various temperatures ($25^\circ C$ ~$95^\circ C$) were examined. Figure 4-3 shows the molecular weights of the silk sericin as defined by SDS-PAGE. As the operating temperature was increased,

the molecular weight was larger. Additional work is needed to evaluate the molecular weight more accurately. When the temperature is high, some of the sericin proteins may be thermally degraded. Figure 4-4 shows the molecular weight of the silk sericin extracted using boiling water at $120^{\circ}C$ in autoclave [48]; the degumming solution was filtered with activated carbon filter in order to remove impurities or precipitates.

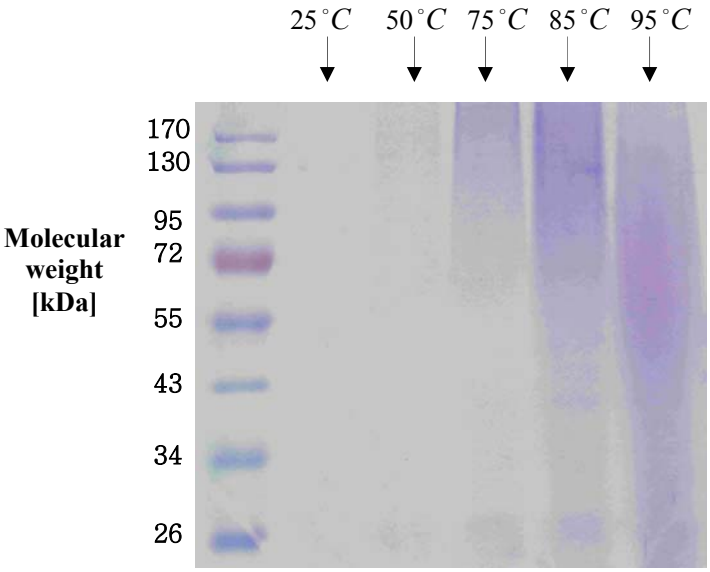

Figure 4-3 SDS-PAGE (10% gel) of silk sericin

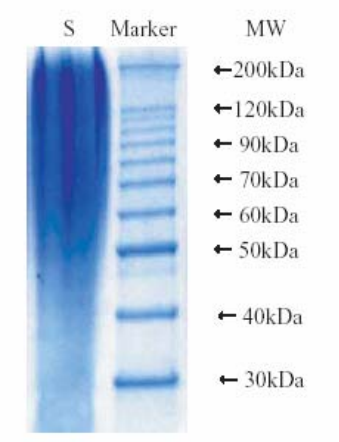

Figure 4-4 SDS-PAGE (12% gel) of silk sericin [48]

4.3 UV/vis spectroscopy

Figure 4-5 shows the absorbance at various wave lengthes. It can be compared with the results (Figure 4-6) of Kato et al. [56] who studied wool fabrics dyed with different natural and chemical dyestuffs. They found that an alkali degummed cocoon sample was removed almost all of the cocoon filament sericin and the sample showed the same level of damage by insect feeding as that of natural cocoons. In their study, the absorption spectra of the solutions, extracted from cocoons treated in different ways, were measured in the wavelength range of 200-700nm. They found that the absorption peak of sericin was at around 280nm, which means the absorption peaks of peptides and amino acids in sericin are at around 280nm. They extracted the sericin by boiling 1 L of water for 1 hour with 20 g of cocoons, and the solution was filtrated through a micro-filter paper (5 and 1.2 μm). Moreover, they also used different extraction methods (such as autoclave, ethanol, and alkali treatment), and the same absorption peak (280nm) of sericin was observed. They reported that using water extraction, there was less damage to the fabrics than using the other chemical treatments (such as enthanol and alkali degumming processes). In this study, the sericin was extracted with water at 35~95$^{\circ}C$ for 6 hours. After extraction and filtration of the sericin solution, the solution was tested for absorption spectra. As shown in Figure 4-5, the silk sericin showed a peak absorbance at around 280nm of wavelength. When the extraction temperature was lower (35 and 50$^{\circ}C$), the absorbance peak at around 280nm was unclear. On the other hand, the peak was more apparent when the temperature was higher (75-95$^{\circ}C$). This may be attributed to the fact at a higher extraction temperature, bigger molecules will be extracted from the cocoon shell.

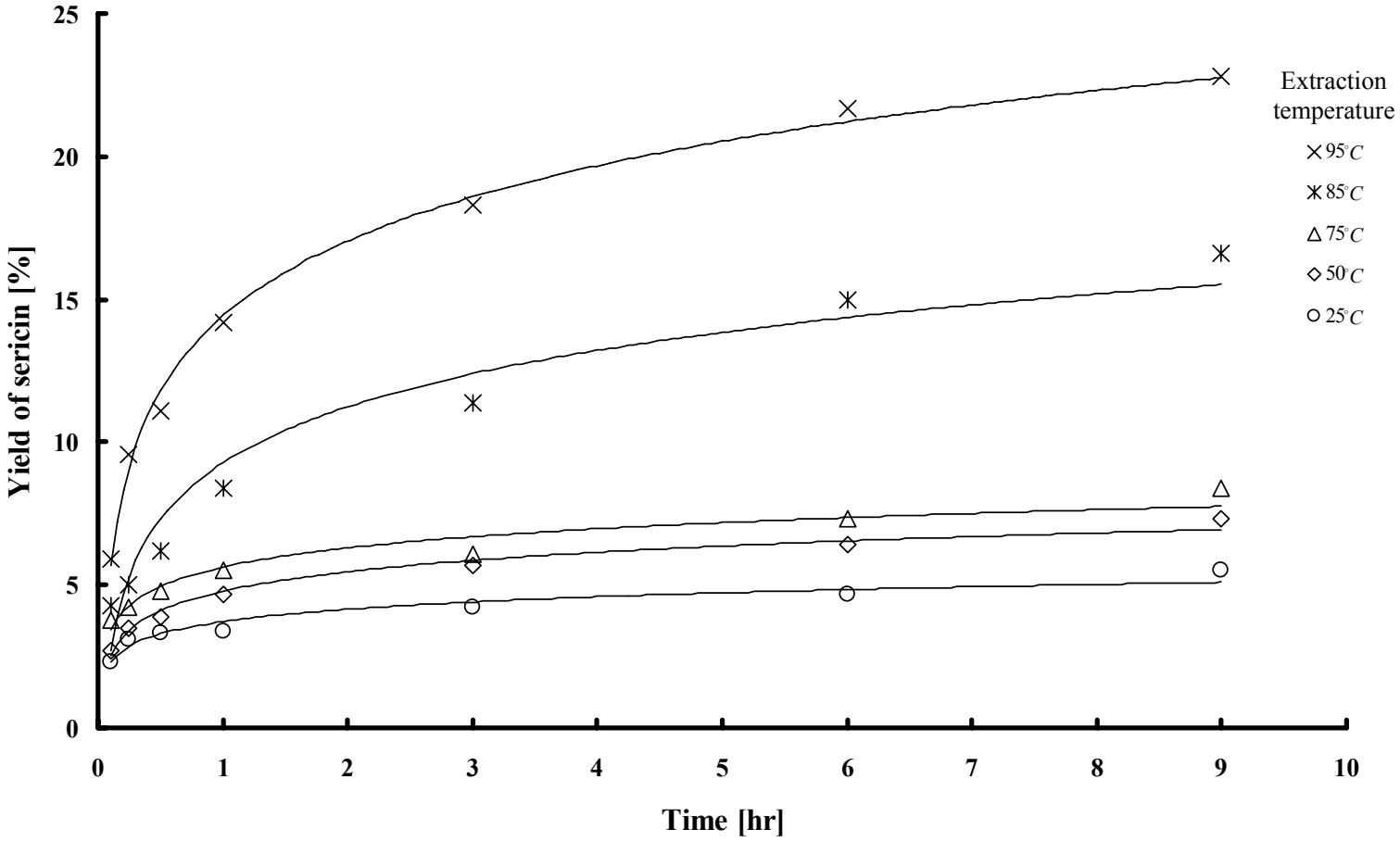

Figure 4-1 Effect of extraction time on the yield of silk sericin at different temperatures

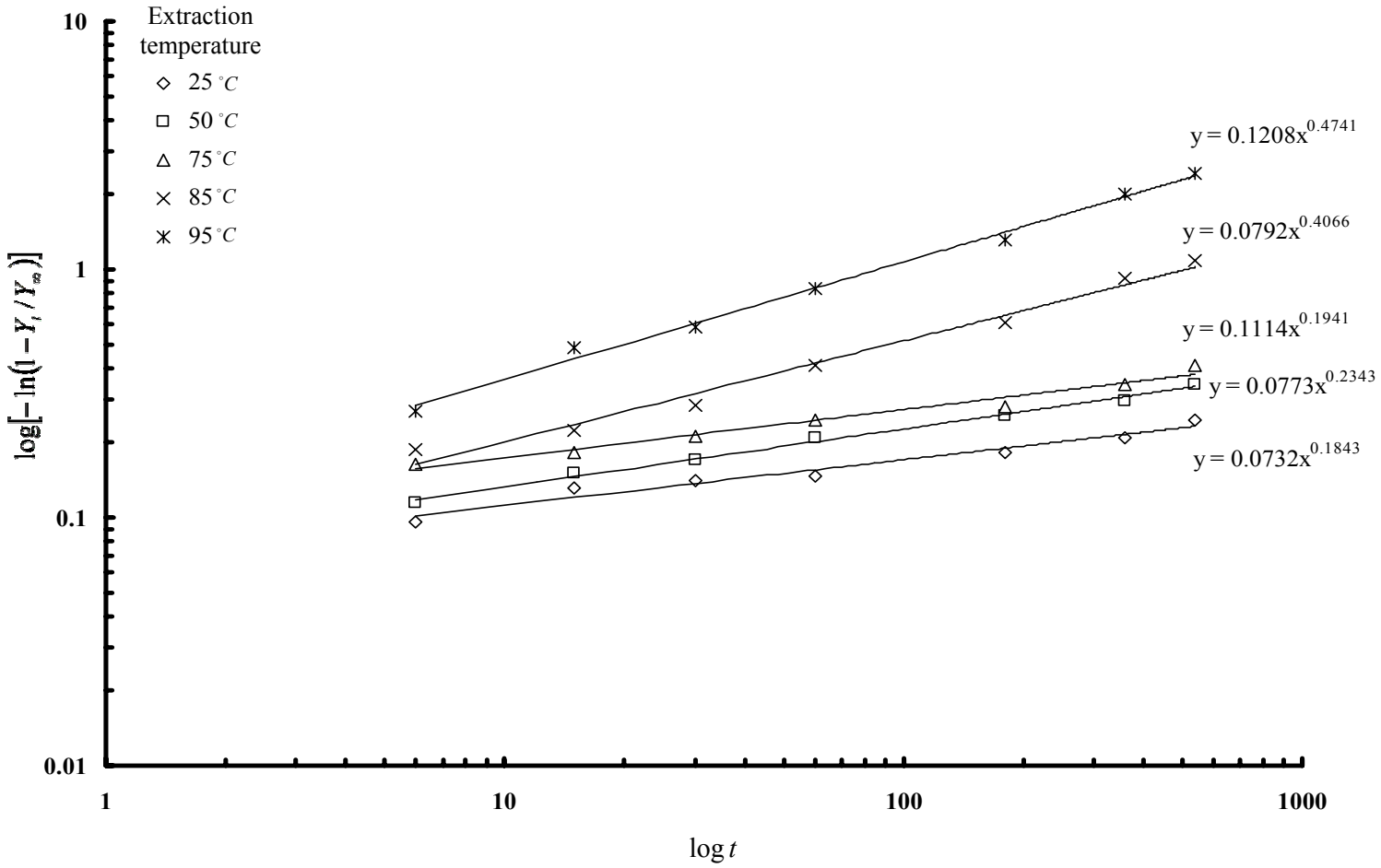

Figure 4-2 Experimental data fitting for yield of silk sericin at different temperatures

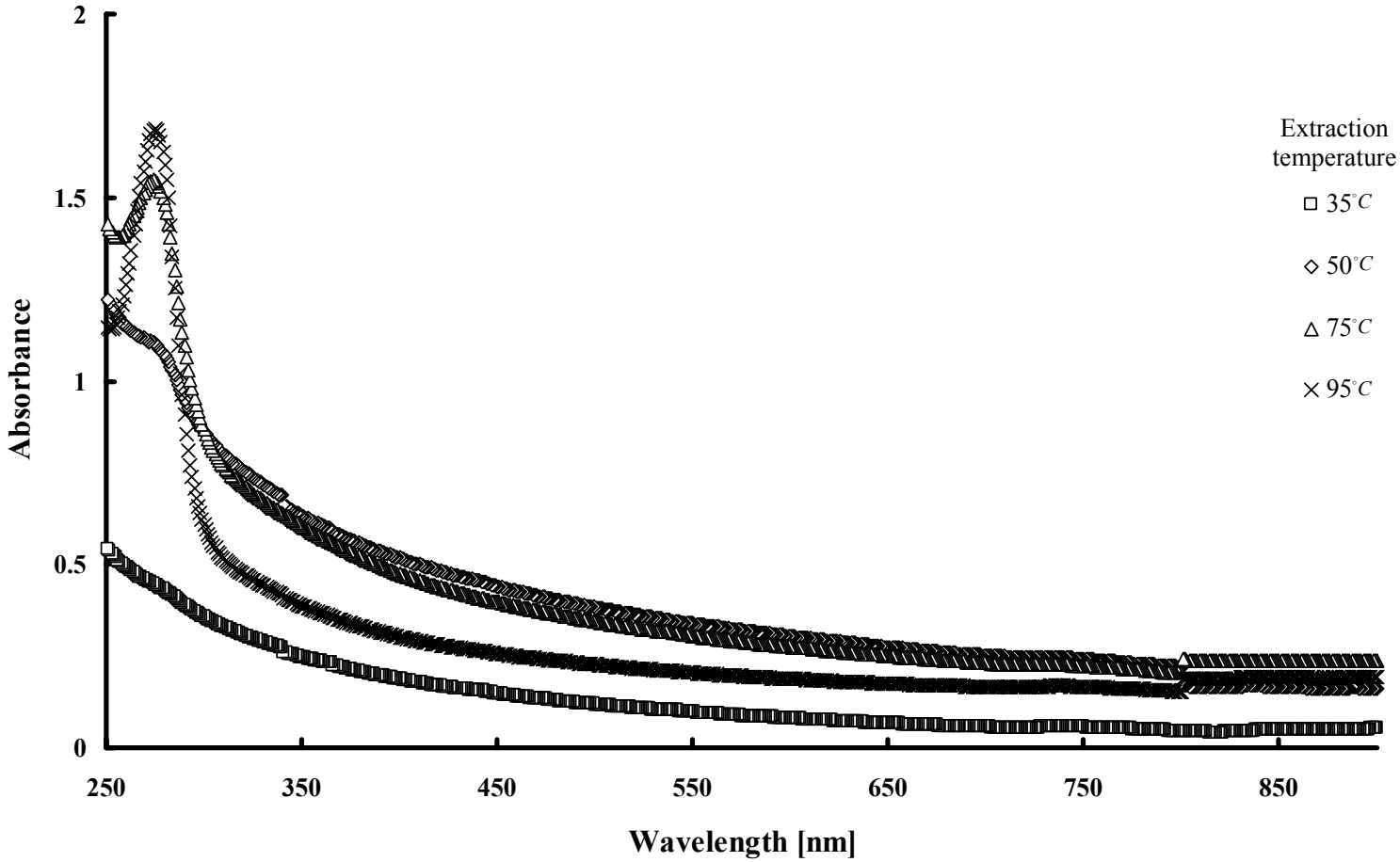

Figure 4-5 Absorption spectra for silk sericin at $35 \sim 95^{\circ}C$ for 9 hr, 1 atm

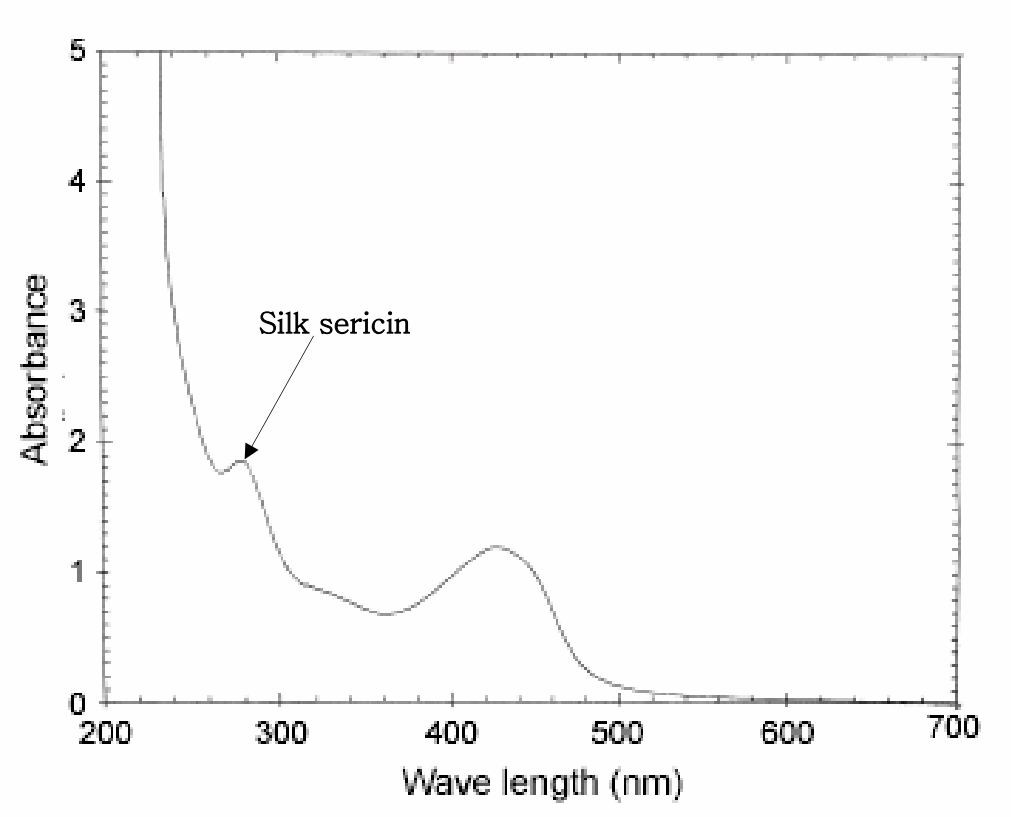

Figure 4-6 Absorption spectrum of cocoon [56]

(The sericin solution was extracted by boiling 1 L of water for 1 hour with 20 g of cocoons.)
(The solution was filtrated through micro-filter papers (5 and 1.2 μm)).

4.4 Membrane crosslinking

The membranes were chemically crosslinked with glutaraldehyde to improve their mechanical strength and chemical stability. The mechanism of chemical crosslinking is discussed below.

Pure PVA membranes

Yeom et al. [70] studied the crosslinking reaction of PVA membranes with glutaraldehyde. In their work, PVA films were crosslinked with different reaction solutions each of which contained a different content of glutaraldehyde (GA) solution, acetone and a catalyst, HCl, to see how the crosslinking agent content affects the pervaporation performance of the membrane to separate acetic acid-water mixtures. The corsslinking reaction between the hydroxyl groups of PVA and the aldehyde groups of glutaraldehyde (GA) was characterized by IR spectroscopy. From IR spectra analysis, it was found that as the glutaraldehyde (GA) solution content in the reaction solution increases, more hydroxyl groups are reacted and more acetal rings and ether linkages are formed. Three possible reaction schemes have been proposed:

PVA + **GA**

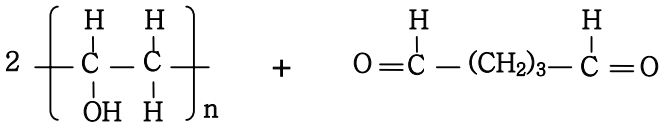

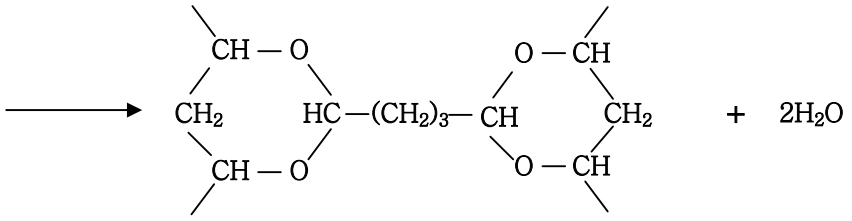

or

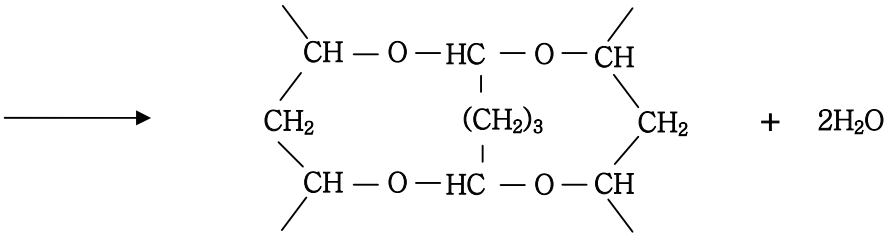

I. Acetal ring group or ether linkage formation

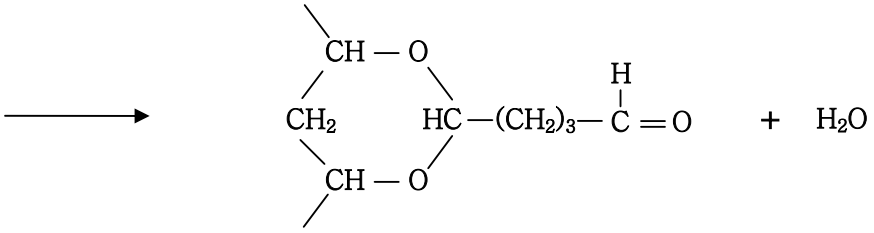

II. Aldehyde formation by monofunctional reaction

Sericin / PVA membranes

The crosslinking reaction of sericin and glutaraldehyde has not been well studied yet because silk sericin has 18 amino acids, which means there may be lots of possible reactions for the crosslinking. Little work can be found in the literature on the crosslinking of sericin. Polypeptides have amine and carboxyl groups at the end of the chain. However, -OH from the carboxyl group at the end of the polypeptide chain can

react with glutaraldehyde. Considering that the hydroxyl groups in PVA are readily crosslinked by glutaraldehyde, it can be thought that the hydroxyl groups in sericin are highly likely to react with the crosslinker. The hypothetical reaction of PVA / sericin blend with glutaraldehyde (GA) is shown below:

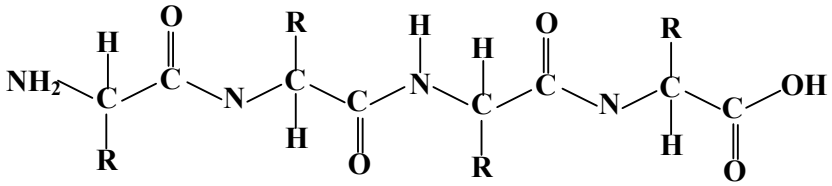

Sericin

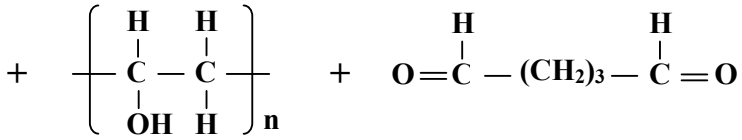

PVA **GA**

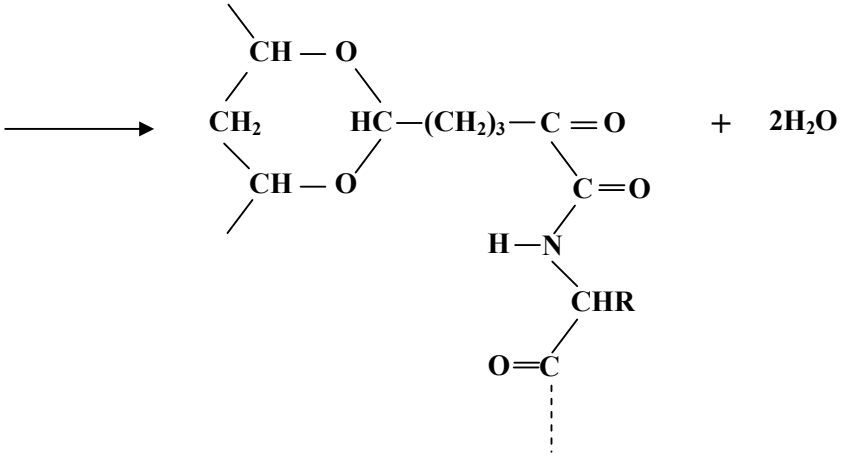

The detailed crosslinking mechanism, which is beyond the scope of the present study, is yet to be determined.

4.5 Permeability and selectivity of pure gases

The sericin / PVA membranes had a thickness in the range of 23-30 μm. Sericin / PVA membranes were tested for permeation of carbon dioxide, oxygen and nitrogen. For the purpose of comparison, membrane permeability (which is a thickness-normalized quantity) was evaluated. In addition, pure PVA membranes were also evaluated. Pure sericin membranes could not be tested because they were too brittle to use as a membrane for gas permeation. For the sericin / PVA membranes tested, the carbon dioxide permeability was found to increase with an increase in the silk sericin concentration up to 6.6%, as shown in Figure 4-7, and then the CO_2 permeability remained approximately the same when sericin concentrations were over 6.6%. Figures 4-8 and 4-9 show, respectively, the permeabilities of nitrogen and oxygen. Similar trends as carbon dioxide permeation were observed. It can be thought that the free volume in water-swollen sericin / PVA membranes increased with increasing sericin concentrations in the membranes since water made the polymer chains more flexible. Free volume is the fraction of total polymer volume which is unoccupied by polymer molecules. When sericin content is higher than 6.6%, the free volume does not seem to increase any more, as will be judged based on the swelling data shown latter. Lin et al. [71] investigated the effect of changing the upstream pressure for permeability of pure gas through poly(ethylene oxide) membranes. The permeability of carbon dioxide and oxygen increase with pressure, indicating plasticization of the membrane, while on the other hand, nitrogen permeability decreases slightly with increasing pressure, as expected from the dual-mode sorption model. However, plasticization refers to an increase in penetrant diffusivity due to the increased polymer local segmental motion caused by the presence of penetrant molecules in the polymer matrix. [26] As penetrant

pressure increases, the tendency of plasticization in a polymer matrix increases, particularly for strongly sorbing penetrants (e.g. carbon dioxide). A high penetrant pressure acting on the membrane can slightly compress the polymer matrix so that the amount of the free volume available for penetrant transport can be reduced. Therefore, the diffusion coefficient is reduced as well. In this study, for the permeation of carbon dioxide and oxygen through the sericin / PVA membranes, the gas permeability slightly increased with an increase in the feed pressure. On the other hand, as shown in Figure 4-8, the nitrogen permeance is slightly reduced when the pressure differential (30-60psi) is increased. It can be thought that when the larger pressure differential is applied to the polymer membrane, the polymer matrix is slightly compressed and the amount of free volume available for penetrate transport is reduced so that the permeability of nitrogen is decreased as a higher pressure is applied.

The selectivity is defined as the ratio of the individual gas permeabilities. Figures 4-10 and 4-11 show the CO_2/N_2 and O_2/N_2 selectivities of the membrane with different sericin / PVA compositions. The selectivity is the ability of the membrane material to separate one component from the others. The results obtained with the pure PVA membrane and with the sericin / PVA membranes are not much different. It seems that the sericin contents did not affect the selectivity of CO_2/N_2 and O_2/N_2 significantly even though the permeability of the pure gases is influenced by the membrane composition. As the penetrant pressure is increased, the selectivity of gases is increased, as shown in Figures 4-10 and 4-11. Adding sericin in the membrane helps speed up humidification and swelling of the membrane because of the excellent moisture retention properties of sericin. This aspect was studied further in the following work on membrane swelling and water uptake rate.

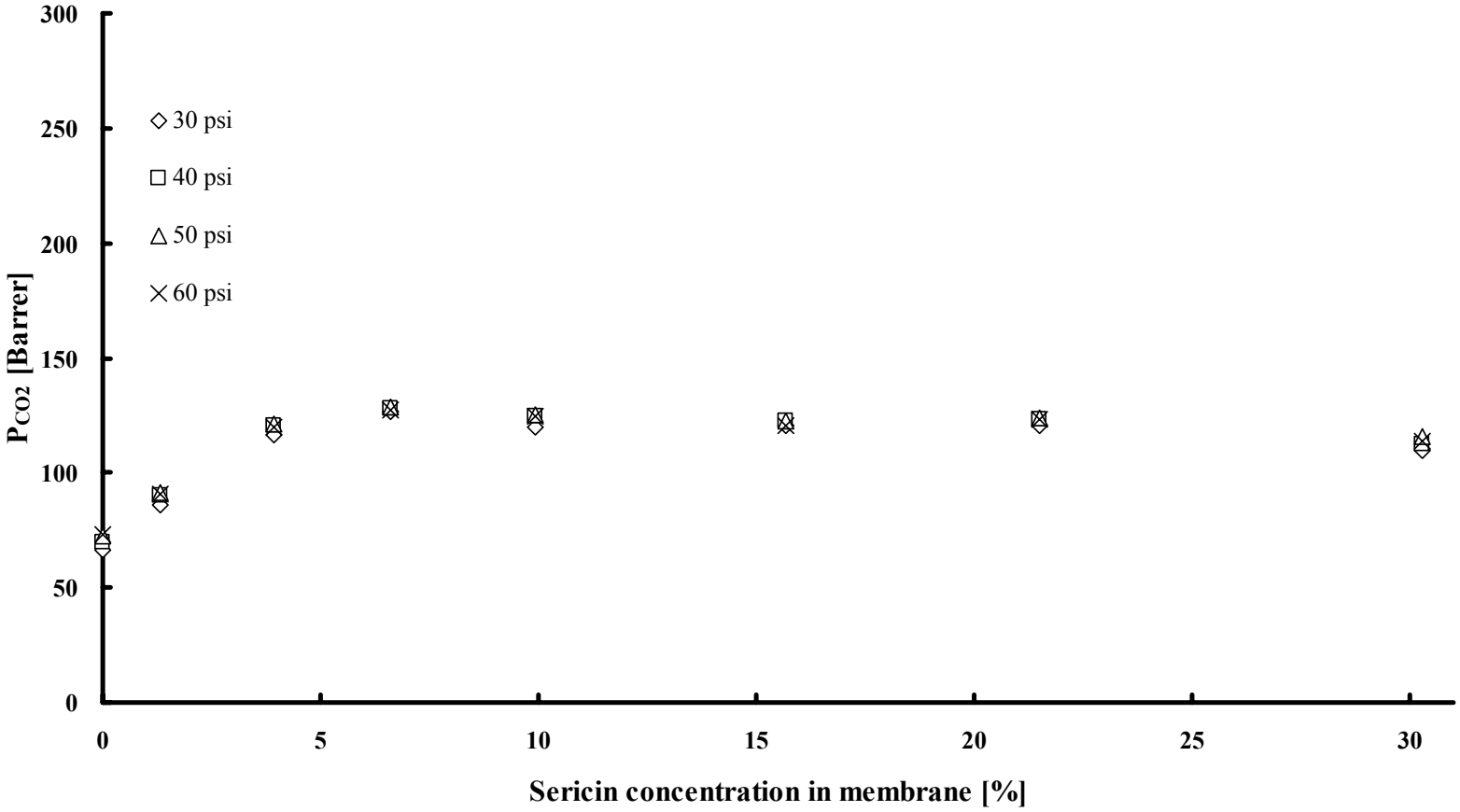

Figure 4-7 Permeability of carbon dioxide at $25^{\circ}C$, 30-60 psi. Membrane thickness $23 \sim 30 \mu m$.

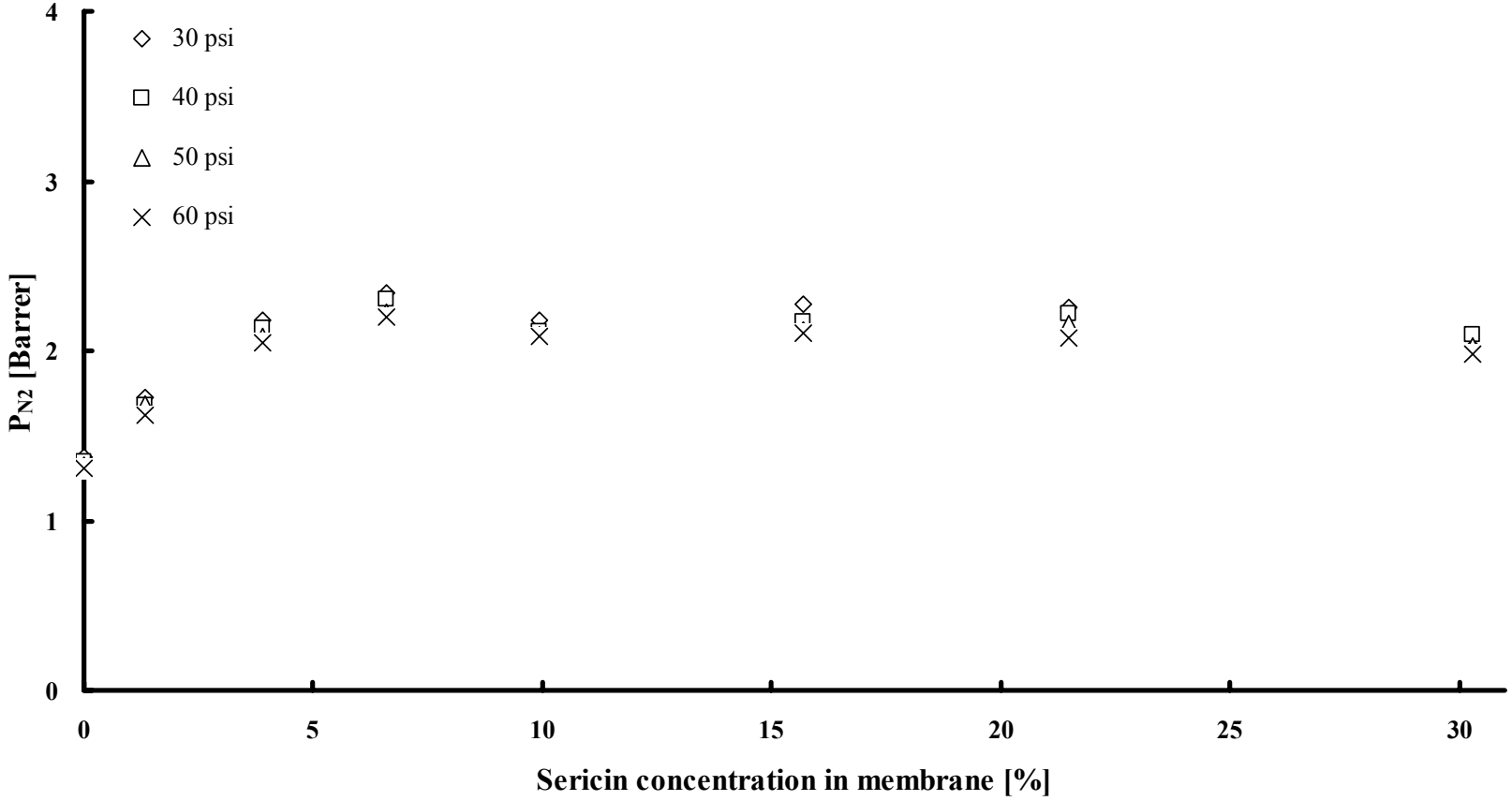

Figure 4-8 Permeability of nitrogen at $25^{\circ}C$, 30-60 psi. Membrane thickness $23 \sim 30 \mu m$.

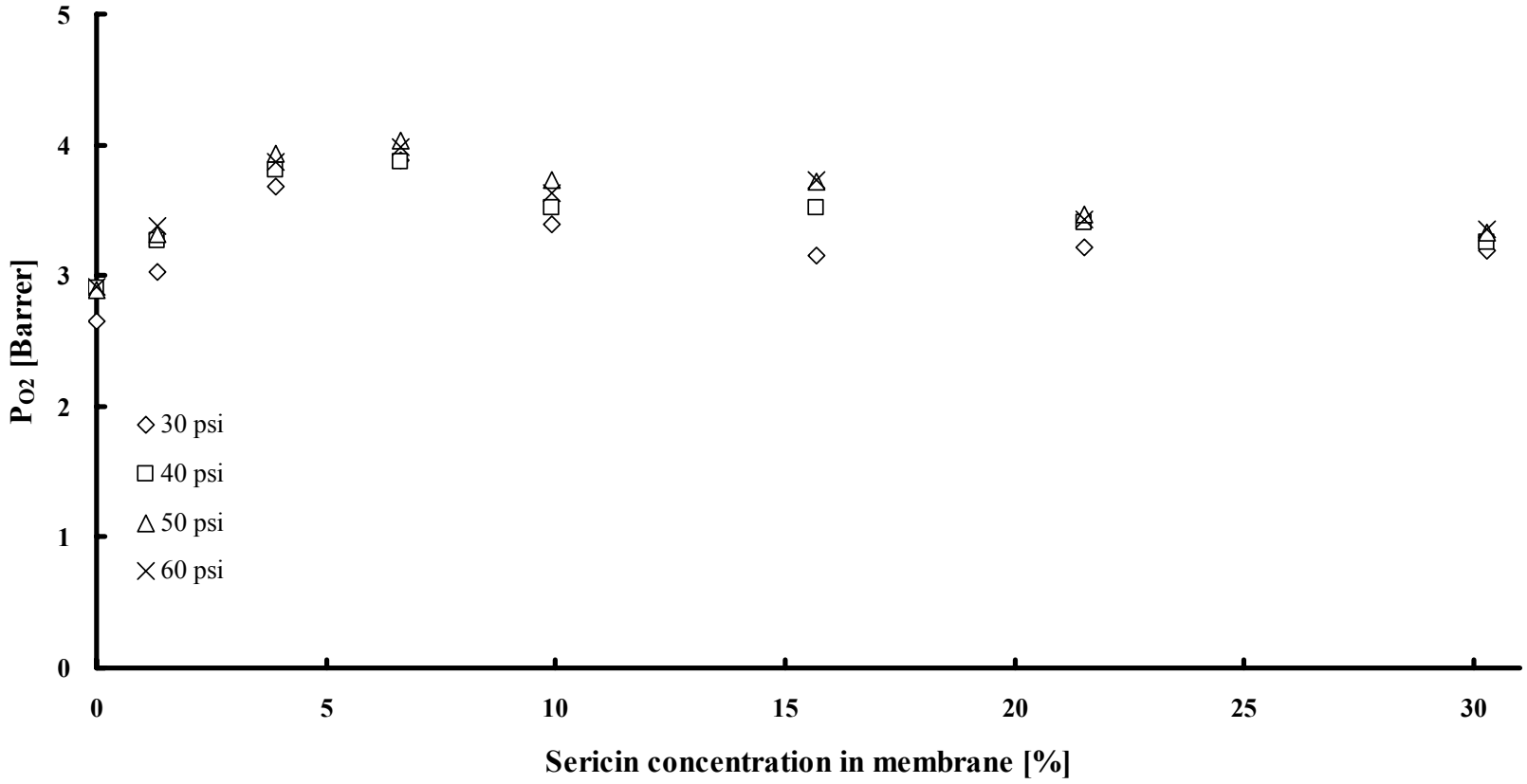

Figure 4-9 Permeability of oxygen at $25^{\circ}C$, 30-60 psi. Membrane thickness $23 \sim 30 \mu m$.

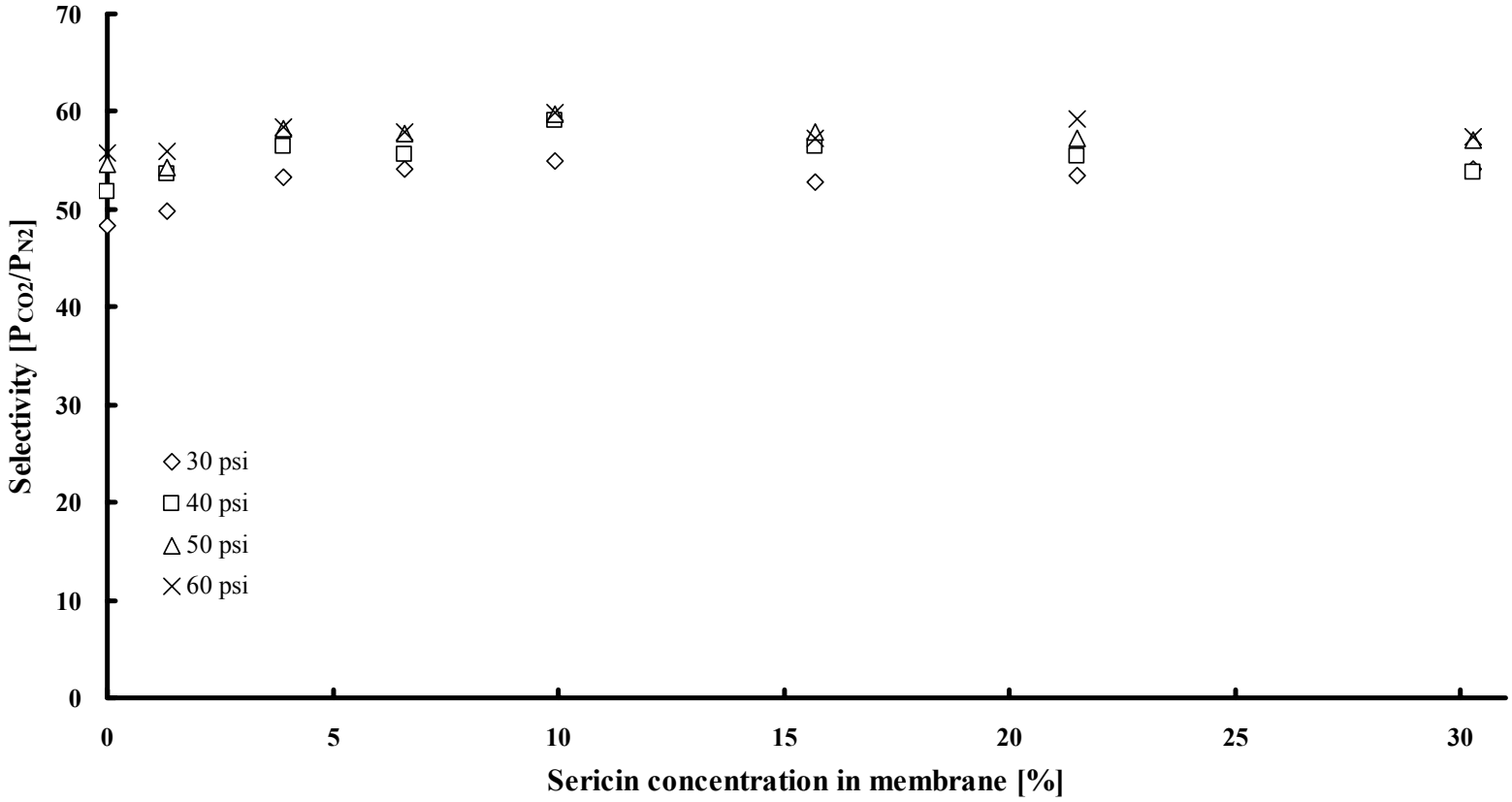

Figure 4-10 Selectivity of carbon dioxide and nitrogen at $25^{\circ}C$, 30-60 psi. Membrane thickness $23 \sim 30 \mu m$.

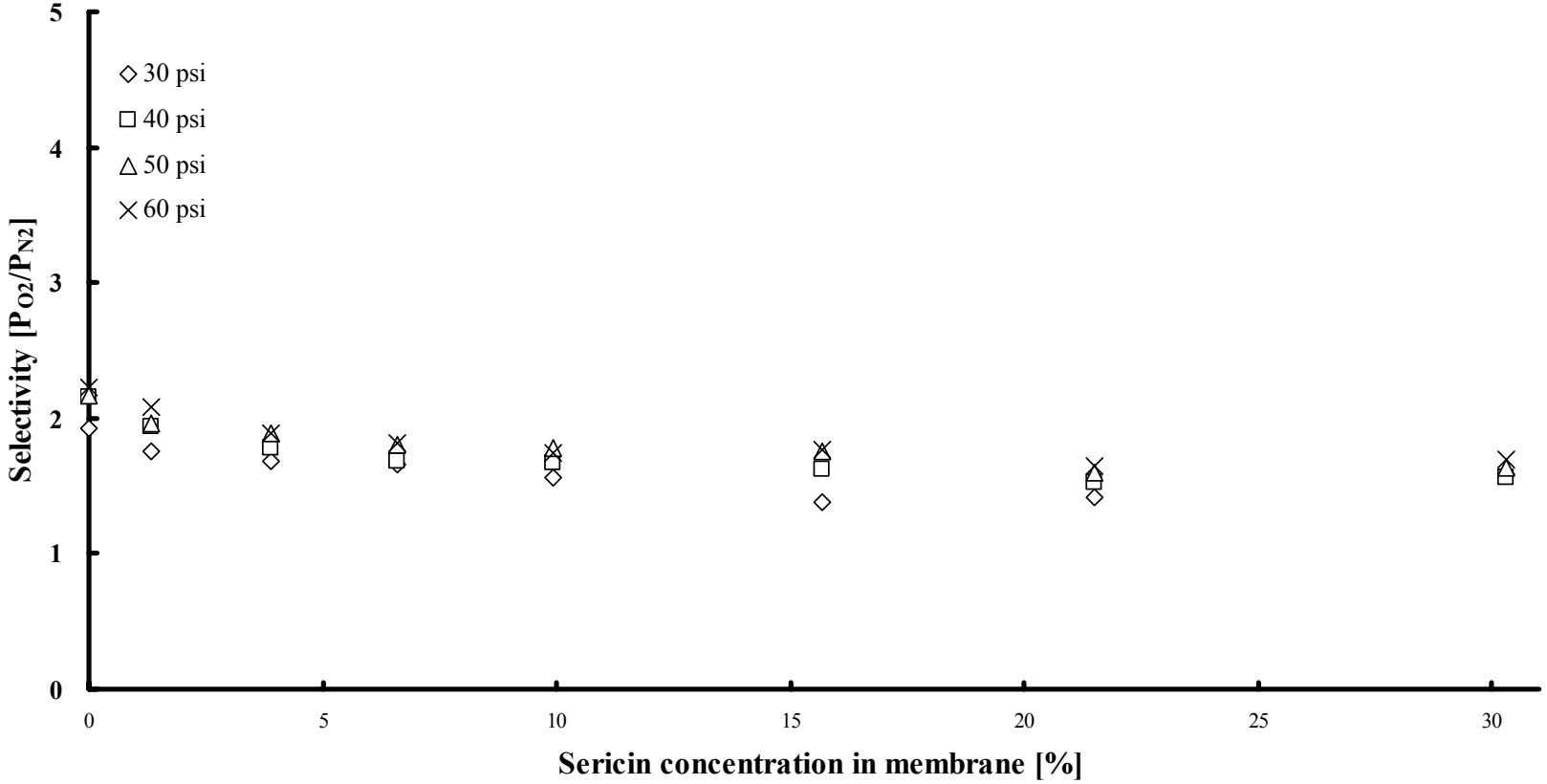

Figure 4-11 Selectivity of oxygen and nitrogen at $25^{\circ}C$, 30-60 psi. Membrane thickness $23 \sim 30 \mu m$.

4. 6 Effects of water in sericin / PVA membranes

Swelling ratio

When water sorbs to the membrane, water molecules diffuse to the inside and cause membrane swelling. The hydroxyl groups of PVA chains and the carboxyl and hydroxyl groups of sericin contribute to the excellent hydrophilicity of the membrane. The addition of water in the polymer matrix increases the segmental mobility of the polymer and free-volume within the structure. As a result, the gas transport is enhanced with membrane swelling. The significantly high permeability of the sericin-containing membrane in water-wet state is due to the membrane swelling. Figure 4-12 shows the swelling ratio of sericin / PVA membranes at different sericin contents. The swelling ratio increased with an increase in the sericin content in the membrane until the sericin concentration reached about 6.6%, thereafter the swelling ratio remained the same. Probably at this concentration, the polymer matrix is completely stretched.

In addition, it is worth noting that the membrane swelling was observed to be extremely fast; water sorption equilibrium can be reached soon after immersing the membrane in water. In fact the sorption rate is so fast that the membrane swells as soon as contacting water. For this reason, water vapor sorption/desorption experiments were conducted to evaluate the diffusivity of water molecules in the membrane.

Water vapor sorption and desorption

It was found that water in the swollen membrane plays an important role in the gas transport. When the membrane is swollen by water, the permeant as a dispersed component can move to and swell the membrane so that gases can permeate through

membrane. Water is a good swelling agent and possibly a moving carrier for the gases (especially CO_2). The mobility of water in the membrane is of interest to study. Water vapor sorption and desorption of the membranes were studied and the diffusion coefficient of water in the membrane could be calculated from the experimental data. The kinetics of water vapor sorption and desorption in the sericin / PVA membranes are shown in Figures 4-13 - 4-14, respectively. The plots of M_t / M_∞ versus $t^{1/2} / l$ for both the sorption and desorption can be drawn on a single graph to compare with water vapor sorption and desorption rates, as shown in Figure 4-15. It can be seen that the water vapor desorption rate is much faster than the sorption rate. This is understandable because of membrane swelling by water molecules. It is expected that as sorption proceeds, the membrane becomes increasingly swollen, leading to an increased diffusivity. The same argument also applies to the desorption process. In general, pure PVA membrane has lower sorption and desorption rates than sericin containing membranes. This may be attributed to the good moisture retention properties of sericin. The diffusion coefficients were evaluated from the sorption and desorption data by fitting equation (3.8) to the experimental data using polymath. The diffusion coefficients so determined are shown in Table 4-2, which shows that the water vapor diffusivity in pure PVA membrane is smaller than that in the sericin-containing PVA membranes. This is more clearly shown in Figure 4-16 where the diffusivity coefficient of water vapor in the membrane is plotted against the sericin content in the membrane.

As mentioned previously, sericin is used as a water retention agent. It can be seen that diffusion coefficients of water vapor in the membrane generally increased when the sericin concentration in the membrane increased. Interestingly, the diffusion coefficient determined from both sorption and desorption at 6.6% of sericin concentration appear to

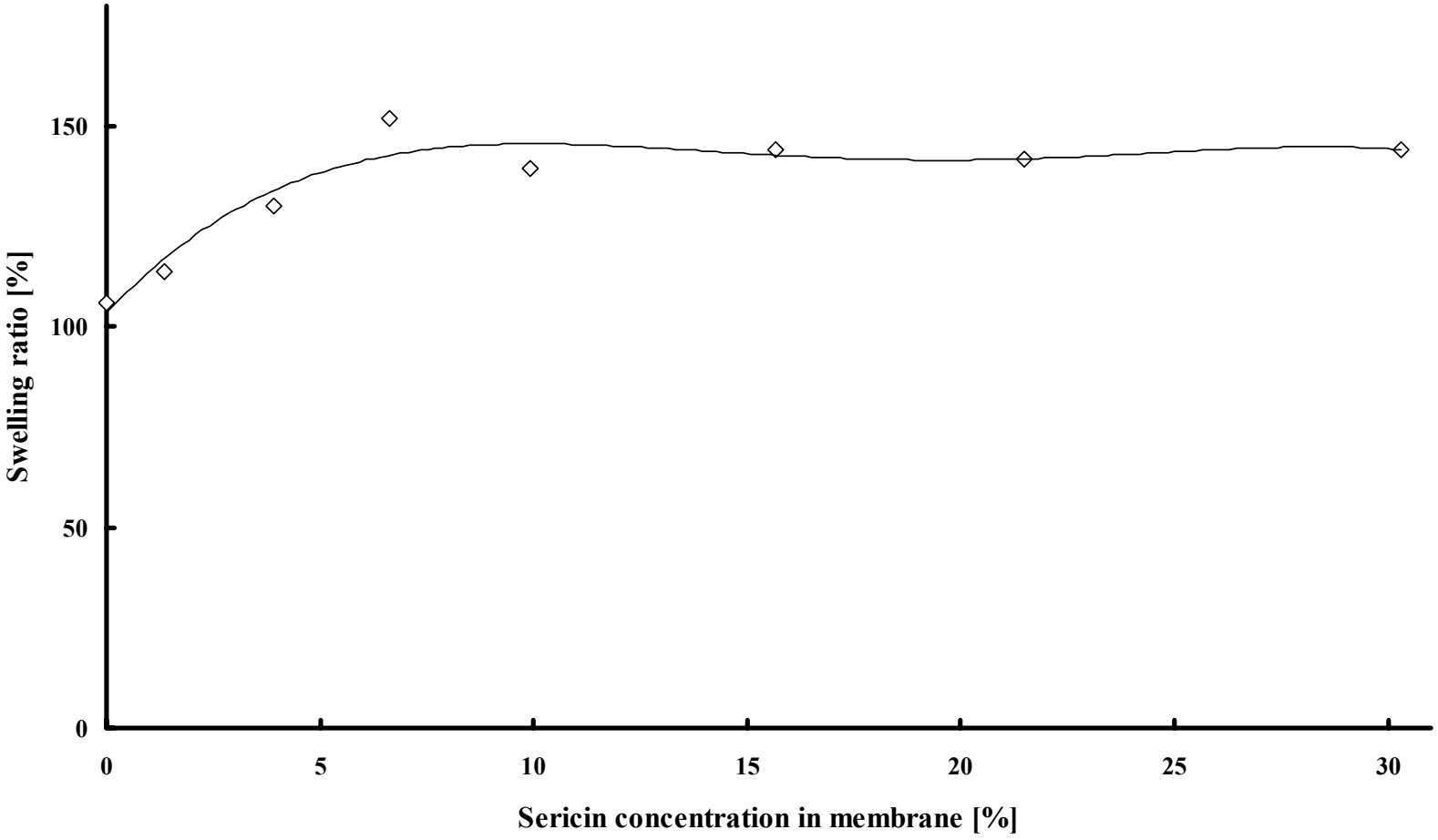

Figure 4-12 Degree of swelling of the membrane in water at $25^{\circ}C$. Membrane thickness $23 \sim 30 \mu m$.

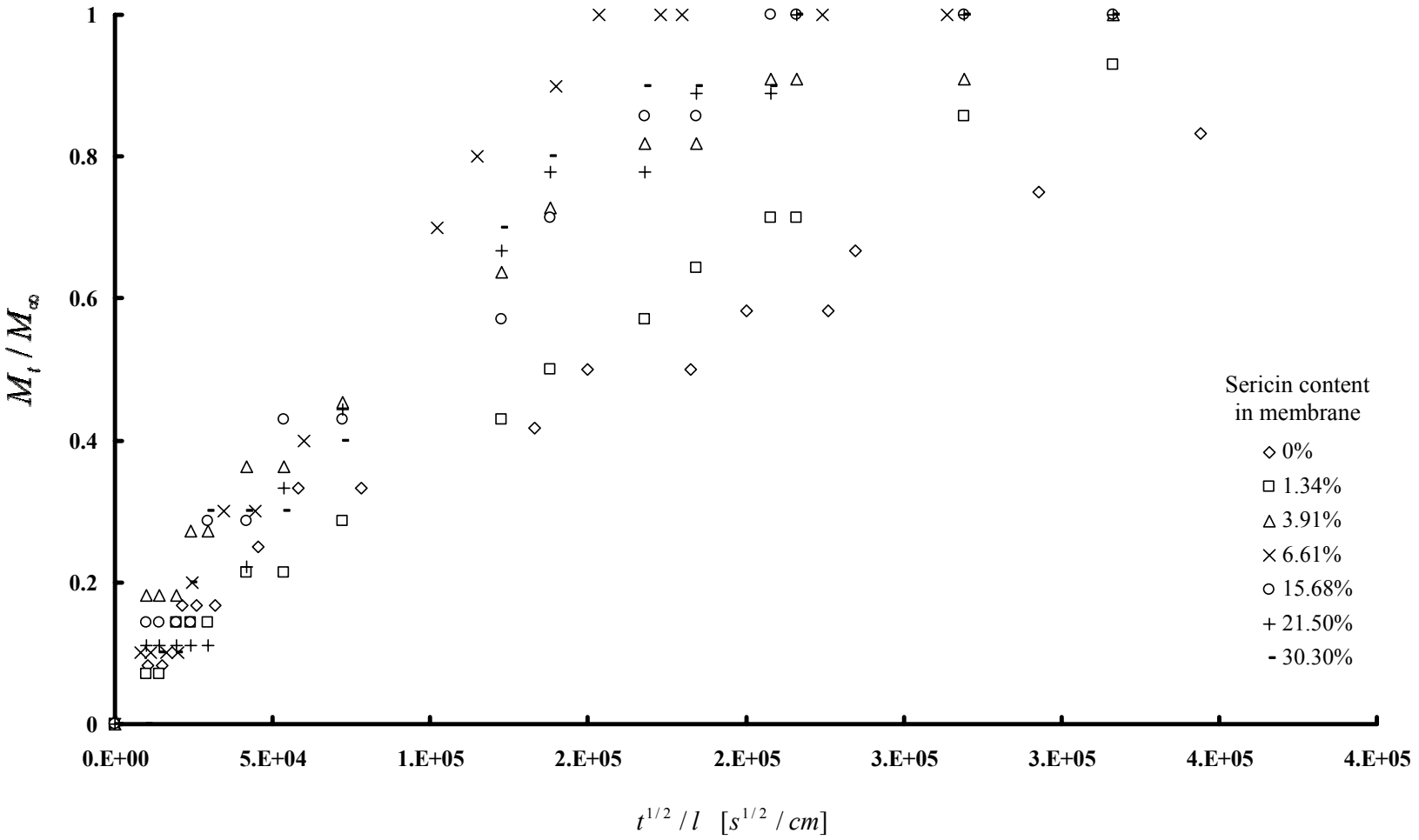

Figure 4-13 Water vapor sorption kinetics at $25^\circ C$. Humidity 55% RH. Membrane thickness $23 \sim 30 \mu m$.

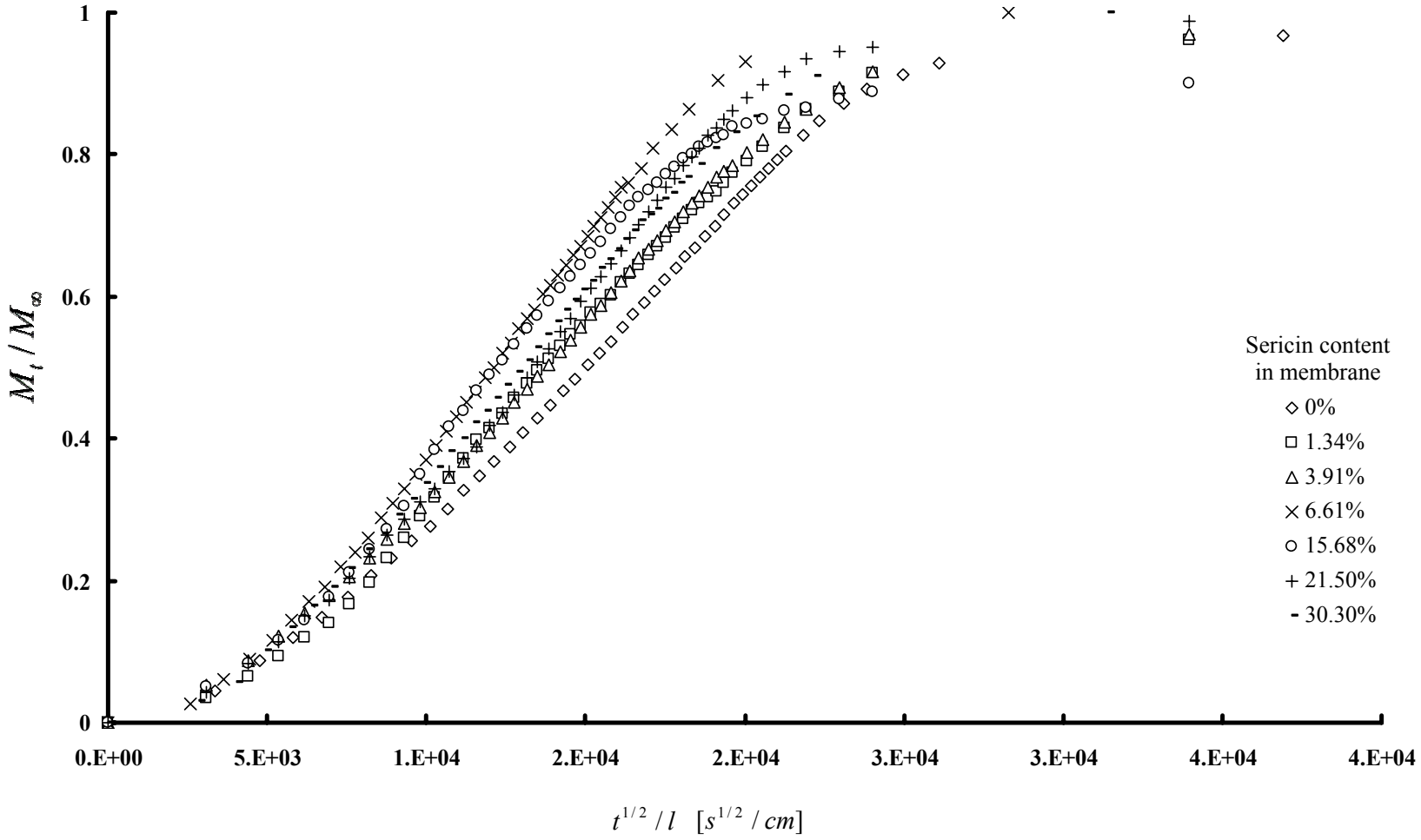

Figure 4-14 Water vapor desorption kinetics at $25\,^{\circ}C$. Humidity 55% RH. Membrane thickness $23 \sim 30 \mu m$.

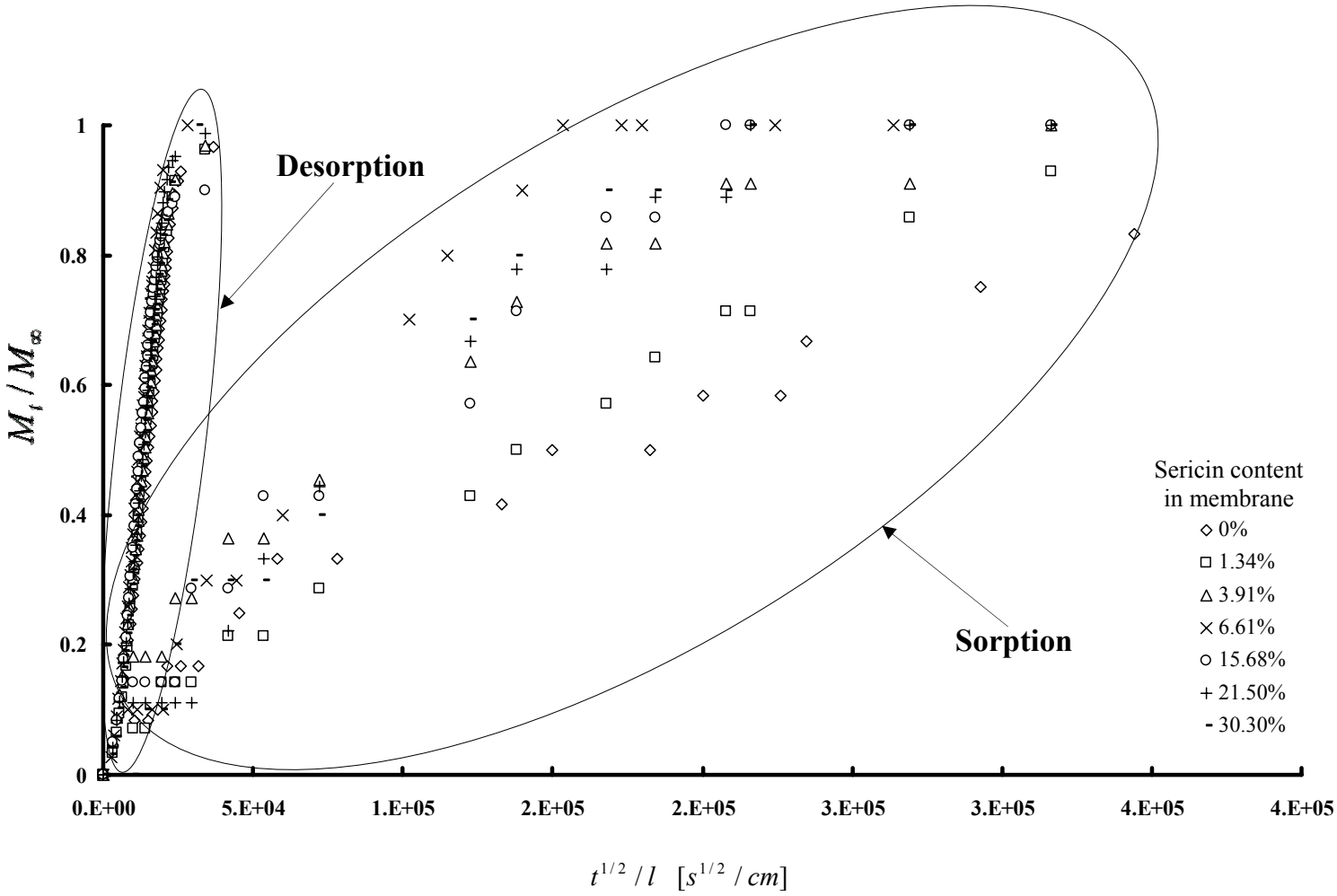

Figure 4-15 Water vapor sorption/desorption at $25^\circ C$, 1atm. Membrane thickness $23 \sim 30 \mu m$.

be the highest. This trend is similar to the swelling ratio. Due to the excellent moisture-absorbing and –desorbing properties of sericin, sericin affects the humidification and swelling of the membrane, and it is clear that water vapor sorption and desorption is related to the swelling of membrane, which in turn affects the gas permselectivity.

Table 4-2 Diffusion coefficient determined from sorption and desporption data using Eqn (3.8)

Sericin concentration in membrane [%]	Membrane thickness [μm]	Diffusivity determined from sorption $D_s \times 10^{12}\ [cm^2/s]$	Diffusivity determined from desorption $D_d \times 10^{12}\ [cm^2/s]$
0%	23	1.7	253
1.3%	25	2.5	285
3.9%	25	2.5	292
6.6%	30	10.7	377
15.7%	25	6.4	363
21.5%	25	6.1	337
30.3%	27	8.3	326

Note that as shown in Figure 4-16, (especially for the sorption data), the M_t / M_∞ vs $\sqrt{t}$ data do not follow a strict linear relationship in the early stage. This means the diffusivity coefficient varies as the membrane is gradually saturated with water and becomes swollen. This is why equation (3.9), which is a simplified version of equation (3.8) applicable to early stage of Fickian diffusion with constant diffusivity, was not used to determine the diffusion coefficient. Instead, the more general equation (equation (3.8)) was used to evaluate the diffusivity by data fitting, covering a wide range of

sorption uptake. Therefore, the diffusivity data so obtained are the apparent overall diffusivity. Murray [72, 73] studied water vapor sorption and desorption in ultrathin chitosan films and similar observation can be made.

Sample calculations of the diffusion coefficient using Polymath can be found in Appendix I.

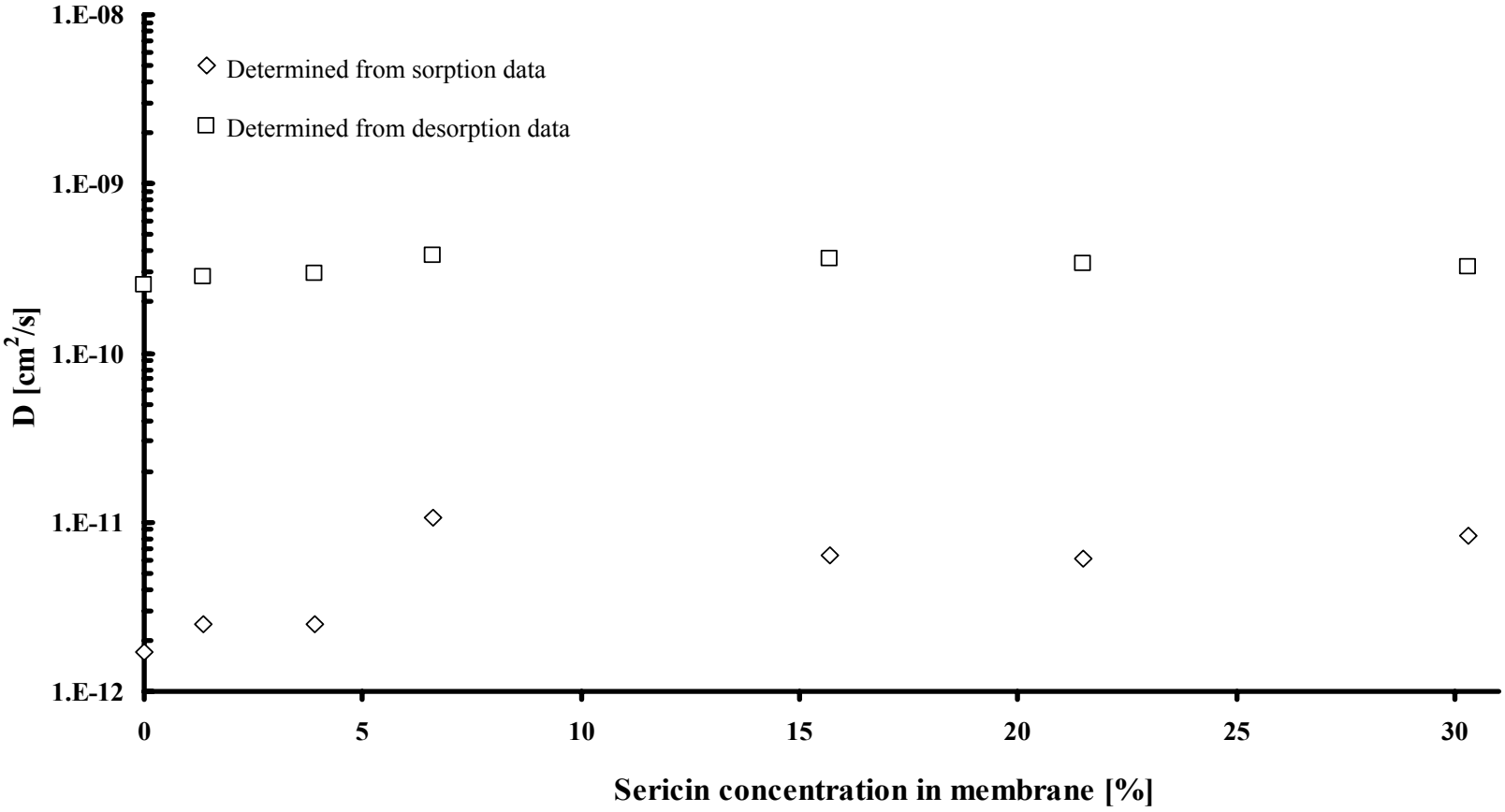

Figure 4-16 Diffusion coefficient of water vapor in membranes containing different amount of sericin. Temperature 25°C.

Chapter 5

Conclusions and recommendations

Conclusions

Extraction of silk sericin from silkworm cocoons was studied. The effect of operating conditions in extraction on the molecular weight of sericin extracted was evaluated. Sericin / PVA membranes were prepared and tested for gas permeation. To our knowledge, this was the first time that sericin was used as a membrane material for gas separation. The following conclusions can be drawn from the studies:

1. Silk sericin can be obtained by extraction with hot water. This is the simplest way to extract sericin from silkworm cocoons.
2. During the extraction, the yield of silk sericin increases with an increase in extraction time and temperature. The highest yield of silk sericin obtained in the study was 22.8%. This means that most silk sericin proteins were extracted. Generally there is 25% of silk sericin in cocoons.
3. Adding 6.6% silk sericin to PVA will increase the membrane permeability. At 6.6%, sericin in the sericin / PVA blend membrane, the permeability of carbon dioxide,

nitrogen and oxygen was 126-129, 1.31-2.34 and 3.9-4.0 Barrer, respectively, and the selectivity of CO_2/N_2 and O_2/N_2 was 54.1-57.9 and 1.7-1.8, respectively.

4. The gas permeability through the membrane increased with an increase in sericin concentration in the membrane until the sericin content in the membrane reached 6.6%, and thereafter a further increase in sericin content in the membrane did not affect the membrane permselectivity significantly.
5. The high permeability of the silk sericin-containing membranes was primarily due to the increased membrane swelling.
6. The experiment of water vapor sorption and desorption in the membranes was tested and the diffusion coefficient was determined. It was shown that water vapor diffusivity during desorption from a pre-saturated membrane was much higher than the diffusivity during sorption into a pre-dried membrane.

Recommendations

The following are recommended for further investigation:

1. Different silk sericin extraction methods should be evaluated to compare with water-treatment method. The molecular weights and extraction yield of sericin by using the different extraction methods may be different.
2. By controlling the conditions such as pH and temperature, the molecular weight of silk sericin could show clear bands in SDS-PAGE. Constituents of amino acids of silk sericin should be evaluated by amino acid analysis.
3. Filtration of silk sericin solution after the extraction should be carried out using, for example, ultrafiltration and microfiltration membrane processes to fractionate the

sericin proteins. Using sericin components with a narrow molecular weight distribution is expected to improve the sericin / PVA membrane properties.

4. The reaction mechanism of sericin, PVA and glutaraldehyde should be studied to better understand the network structure of the sericin / PVA blend membranes.
5. Experiments with mixture gases may be carried out, especially for CO_2/N_2 system where the membrane showed favorable permselectivity, in order to investigate the membrane potential for real applications.
6. Effect of diffusivity and solubility of carbon dioxide, oxygen and nitrogen in water-swollen sericin / PVA membranes should be investigated in order to get an insight into the transport mechanism.

Bibliography

[1] A. Figoli, W. Sager and M. Mulder, Facilitated oxygen transport in liquid membranes: review and new concepts, Journal of Membrane Science 181 (2001) 97-110

[2] W. J. Koros and G. K. Fleming, Membrane-based gas separation, Journal of Membrane Science 83 (1993) 1-80

[3] M. J. Kim, Y. I. Park, K. H. Youm and K. H. Lee, Gas permeation through water-swollen polysaccharide/poly(vinyl alcohol) membranes, Journal of Applied Polymer Science 91 (2004) 3225-3232

[4] R. W. Baker, Membrane Technology and Applications, John Wiley & Sons 2004

[5] M. Mulder, Basic Principles of Membrane Technology 2nd ed., Kluwer Academic Publishers 1998

[6] A. Javaid, Membranes for solubility-based gas separation applications, Chemical Engineering Journal 112 (2005) 219-226

[7] W. J. Ward, Analytical and experimental studies of facilitated transport, AIChE Journal 16 (1970) 405-410

[8] T. L. Donaldson and J. A. Quinn, Carbon dioxide transport through enzymatically active synthetic membranes, Chemical Engineering Science 30 (1975) 103-115

[9] A. Basu, J. Akhtar, M. H. Rahman and M. R. Islam, A review of separation of gases using membrane systems, Petroleum Science and Technology 22 (2004) 1343-1368

[10] D. R. Smith and J. A. Quinn, The prediction of facilitation factors for reaction augmented membrane transport, AIChE Journal 25 (1979) 197-200

[11] J. H. Meldon, Y. Kang and N. Sung, Analysis of transient permeation through a membrane with immobilizing chemical reaction, Industrial and Engineering Chemistry Fundamentals 24 (1985) 61-64

[12] H. Matsuyama, M. Teramoto, K. Matsui and Y. Kitamura, Preparation of poly(acrylic acid)/poly(vinyl alcohol) membrane for the facilitated transport of CO_2, Journal of Applied Polymer Science 81 (2001) 936-942

[13] M. Teramoto, Q. Huang, T. Watari, Y. Tokunaga, R. Nakatani, T. Maeda and H. Matsuyama, Facilitated transport of CO_2 through supported liquid membranes of various amine solutions - effects of rate and equilibrium of reaction between CO_2 and amine, Journal of Chemical Engineering of Japan 30 (1997) 328-335

[14] A. S. Kovvali and K. K. Sirkar, Carbon dioxide separation with novel solvents as liquid membranes, Industrial and Engineering Chemistry Research 41 (2002) 2287-2295

[15] P. F. Scholander, Oxygen transport through hemoglobin solutions, Science 131 (1960) 585-590

[16] R. J. Bassett and J. S. Schultz, Nonequilibrium facilitated diffusion of oxygen through membranes of aqueous cobaltodihistidine, Biochimica et Biophysica Acta 211 (1970) 194-215

[17] B. M. Johnson, R. W. Baker, S. L. Matson, K. L. Smith, I. C. Roman, M. E. Tuttle and H. K. Lonsdale, Liquid membranes for the production of oxygen-enriched air. II. Facilitated-transport membranes, Journal of Membrane Science 31 (1987) 31-67

[18] H. Nishide, H. Kawakami, T. Suzuki, Y. Azechi and E. Tsuchida, Enhanced satbility and facilitation in the oxygen transport through cobalt porphyrin polymer

membranes, Macromolecules 23 (1990) 3714-3716

[19] H. Fujita, Diffusion in polymer-diluent system, Fortschr. Hochpolym. Forsch. 3 (1961) 1-47

[20] J. S. Vrentas, Diffusion in polymer-solvent systems. II. A predictive theory for the dependence of diffusion coefficients on temperature, concentration, and molecular weight, Journal of Polymer Science 15 (1977) 417-439

[21] T. P. Lodge, J. A. Lee and T. S. Frick, Probe diffusion in poly(vinyl acetate)/toluene solutions, Journal of Polymer Science: Part B: Polymer Physics 28 (1990) 2607-2627

[22] J. S. Vrentas and C. M. Vrentas, Evaluation of free-volume theories for solvent self-diffusion in polymer-solvent systems, Journal of Polymer Science: Part B: Polymer Physics 31 (1993) 69-76

[23] T. S. Frick, W. J. Huang, M. Tirrell and T. P. Lodge, Probe diffusion in polystyrene/toluene solutions, Journal of Polymer Science: Part B: Polymer Physics 28 (1990) 2629-2649

[24] S. A. Stern and W. J. Koros, Separation of gas mixtures with polymer membrane. A brief overview, Chimie Nouvelle 18 (2000) 3201-3215

[25] L. M. Robeson, Polymer membranes for gas separation, Current Opinion in Solid State and Materials Science 4 (1999) 549-552

[26] T. C. Merkel, V. I. Bondar, K. Nagai, B. D. Freeman and I. Pinnau, Gas sorption, diffusion, and permeation in poly(dimethylsiloxane), Journal of Polymer Science: Part B: Polymer Physics 38 (2000) 415-434

[27] Y. I. Park and K. H. Lee, Preparation of water-swollen hydrogel membranes for gas separation, Journal of Applied Polymer Science 80 (2001) 1785-1791

[28] A. Ito, M. Sato and T. Anma, Permeability of CO_2 through chitosan membrane swollen by water vapor in feed gas, Die Angewandte Makromolekulare Chemie 248 (1997) 85-94

[29] H. Matsuyama, M. Teramoto, H. Sakakura and K. Iwai, Facilitated transport of CO_2 through various ion exchange membranes prepared by plasma graft polymerization, Journal of Membrane Science 117 (1996) 251-260

[30] C. K. Yeom, S. H. Lee and J. M. Lee, Study of transport of pure and mixed CO_2/N_2 gases through polymeric membranes, Journal of Applied Polymer Science 78 (2000) 179-189

[31] H. J. Lehermeier, J. R. Dorgan and J. D. Way, Gas permeation properties of poly(lactic acid), Journal of Membrane Science 190 (2001) 243-251

[32] C. C. Wang, C. Y. Chen, C. C. Huang, C. Y. Chen and J. F. Kuo, Permeation of oxygen/nitrogen in cobalt-chelated copoly(EDTA-MMA-BA) membranes, Journal of Membrane Science 177 (2000) 189-199

[33] A. Morisato and I. Pinnau, Synthesis and gas permeation properties of poly(4-methyl-2-pentyne), Journal of Membrane Science 121 (1996) 243-250

[34] J. P. Rigueiro, M. Elices, J. Llorca and C. Viney, Tensile properties of silkworm silk obtained by forced silking, Journal of Applied Polymer Science 82 (2001) 1928-1935

[35] Y. Shen, M. A. Johnson and D. C. Martin, Microstructural characterization of bombyx mori silk fibers, Marcomolecules 31 (1998) 8857-8864

[36] H. Teramoto, A. Kakazu and T. Asakura, Native structure and degradation pattern of silk sericin studied by ^{13}C NMR spectroscopy, Marcomolecules 39 (2006) 6-8

[37] Y. Q. Zhang, Application of natural silk protein sericin in biomaterials,

Biotechnology Advances 20 (2002) 91-100

[38] F. Freddi, R. Mossotti and R. Innocenti, Degumming of silk fabric with several proteases, Journal of Biotechnology 106 (2003) 101-112

[39] Wikipedia, the free encyclopedia, Image : Protein-primary-structure.png, (http://en.wikipedia.org/wiki/Image:Protein-primary-structure.png)

[40] R. T. Morrison, R. N. Boyd, Organic Chemistry 6th ed., Prentice Hall 1992

[41] Y. Q. Zhang, M. L. Tao, W. D. Shen, J. P. Mao and Y. Chen, Synthesis of silk sericin peptides-L-asparaginase bioconjugates and their characterization, Journal of Chemical Thechnology and Biotechnology 81 (2006) 136-145

[42] M. A. Becker, P. Willman and N. C. Tuross, The U.S. first ladies gowns: a biochemical study of silk preservation, Journal of the American Institute for Conservation 34 (1995) 141-152

[43] Assist. Prof. Dr. A. Sonthisombat and Dr. P. T. Speakman, Silk : Queen of fibres – The concise story, Journal of Faculty of Engineering, RIT

[44] W. Tao, M. Li and R. Xie, Preparation and structure of porous silk sericin materials, Macromolecular Materials and Engineering 290 (2005) 188-194

[45] H. Y. Kweon, J. H. Yeo, K. G. Lee, Y. H. Park, J. H. Hahm and C. S. Cho, Effects of poloxamer on the gelation of silk sericin, Macromolecular Rapid Communications 21 (2000) 1302-1305

[46] N. Kato, S. Sato, A. Yamanka, H. Yamada, N. Fuwa and M. Nomura, Silk protein, sericin, inhibits lipid peroxidation and tyrosinase activity, Bioscience, Biotechnology and Biochemistry 62 (1998) 145-147

[47] S. Terada, T. Nishimura, M. Sasaki, H. Yamada and M. Miki, Sericin, a protein derived from silkworms, accelerates the proliferation of several mammalian cell

lines including a hybridoma, Cytotechnology 40 (2002) 3-12

[48] Y. Q. Zhang, M. L. Tao, W. D. Shen, Y. Z. Zhou, Y. Ding and W. L. Zhou, Immobilization of L-asparaginase on the microparticles of the natural silk sericin protein and its characters, Biomaterials 25 (2004) 3751-3759

[49] K. Y. Cho, J. Y. Moon, Y. W. Lee, K. G. Lee, J. H. Yeo, H. Y. Kweon, K. H. Kim and C. S. Cho, Preparation of self-assembled silk sericin nanoparticles, International Journal of Biological Macromolecules 32 (2003) 36-42

[50] J. S. Ahn, H. K. Choi, K. H. Lee, J. H. Nahm and C. S. Cho, Novel mucoadhesive polymer prepared by template polymerization of acrylic acid in the presence of silk sericin, Journal of Applied Polymer Science 80 (2001) 274-280

[51] C. Fabiani, M. Pizzichini, M. Spadoni and G. Zeddita, Treatment of waste water from silk degumming processes for protein recovery and water reuse, Desalination 105 (1996) 1-9

[52] K. G. Lee, H. Y. Kweon, J. H. Yeo, S. O. Woo, Y. W. Lee, C. S. Cho, K. H. Kim and Y. H. Park, Effect of methyl alcohol on the morphology and conformational characteristics of silk sericin, Biological Marcomolecules 33 (2003) 75-80

[53] S. Terada, M. Sasaki, K. Yanagihara and H. Yamada, Preparation of silk protein sericin as mitogenic factor for better mammalian cell culture, Journal of Bioscience and Bioengineering 6 (2005) 667-671

[54] K. H. Lee, Silk sericin retards the crystallization of silk fibroin, Macromolecular Rapid Communications 25 (2004) 1792-1796

[55] P. Jiang, H. Liu, C. Wang, L. Wu, J. Huang and C. Guo, Tensile behaviour and morphology of differently degummed silkworm (*Bombyx mori*) cocoon silk fibers, Materials Letters 60 (2006) 919-925

[56] H. Kato, T. Hata and M. Tsukada, Potentialities of natural dyestuffs as antifeedants against varied carpet beetle, *Anthrenus verbasci*, Japan Agricultural Research Quarterly 38 (2004) 241-251

[57] M. Takahashi, K. Tsujimoto, H. Yamada, H. Takagi and S. Nakamori, The silk protein, sericin, protects against cell death caused by acute serum deprivation in insect cell culture, Biotechnology Letters 25 (2003) 1805-1809

[58] H. Yamada, H. Nakao, Y. Takasu and K. Tsubouchi, Preparation of undegraded native molecular fibroin solution from silkworm cocoons, Materials Science and Engineering 14 (2001) 21-46

[59] I. Cho and K. K. Kim, Graft copolymerization to proteins (II). Separation and purification of sericin, and its graft copolymerization with acrylonitrile, Journal of the Korean Chemical Society 20 (1976) 309-315

[60] L. K. Hazarika, C. N. Saikia, A. Kataky, S. Bordoloi and J. Hazarika, Evaluation of physico chemical characteristics of silk fibres of antheraea assama reared on different host plants, Bioresource Technology 64 (1998) 67-70

[61] A. L. Lehninger, Biochemistry 3rd ed., Worth Publishers 1971

[62] J. Huang, R. Valluzzi, E. Bini, B. Vernaglia and D. L. Kaplan, Cloning, expression, and assembly of sericin-like protein, Journal of Biological Chemistry 278 (2003) 46117-46123

[63] K. H. Lee, Application of silk sericin as a polymer material, Polymer (Korea) 16 (2005) 577-587

[64] J. Teramoto and M. Miyazawa, Molecular orientation behaviour of silk sericin film as revealed by ATR infrared spectroscopy, Biomacromolecules 6 (2005) 2049-2057

[65] H. Miyake, H. Wakisaka and M. Nagura, Structures and physical properties of poly(vinyl alcohol)/sericin blended plastic, Journal of Insect Biotechnology and Sericology 71 (2002) 85-89

[66] U. K. Laemmli, Cleavage of structural proteins during the assembly of the head of bacteriophage T4, Nature 227 (1970) 680

[67] H. Kumar and Siddaramaiah, A study of sorption/desorption and diffusion of substititued aromatic probe molecules into semi interpenetrating polymer network of polyurethane/polymethyl methacrylate, Polymer 46 (2005) 7140-7155

[68] T. Watari, H. Wang, K. Kuwahara, K. Tanaka, H. Kita and K. Okamoto, Water vapor sorption and diffusion properties of sulfonated polyimide membranes, Journal of Membrane Science 219 (2003) 137-147

[69] P. P. Roussis, Diffusion of water vapour in polymethyl methacrylate, Journal of Membrane Science 15 (1983) 141-155

[70] C. K. Yeom and K. H. Lee, Pervaporation separation of water-acetic acid mixtures through poly(vinyl alcohol) membranes crosslinked with glutaraldehyde, Journal of Membrane Science 109 (1996) 257-265

[71] H. Lin and B. D. Freeman, Gas solubility, diffusivity and permeability in poly(ethylene oxide), Journal of Membrane Science 239 (2004) 105-117

[72] C. Murray, The effects of heating and chemical acetylation on ultrathin chitosan films, PhD Thesis, University of Guelph, 2007

[73] C. A. Murray and J. R. Dutcher, Effect of changes in relative humidity and temperature on ultrathin chitosan films, Biomacromolecules 7 (2006) 3460-3465

List of symbols

A	Area of permeation	$[cm^2]$
C	Concentration	$[mole/cm]$
D	Diffusion coefficient	$[cm^2/s]$
E_d	Activation energy of diffusion	$[J/mole]$
E_p	Activation energy of permeation	$[J/mole]$
F	Permeation rate	$[cm^3/s]$
J	Flux	$[cm/s]$
l	Membrane thickness	$[cm]$
M_t	Weight change of membrane at time t	$[g]$
M_∞	Weight of membrane at equilibrium	$[g]$
P	Permeability	$[cm^3(STP)\cdot cm/cm^2\cdot s\cdot cmHg]$
p	Partial pressure	$[cmHg]$
S	Solubility coefficient	$[cm^3/cm^3\cdot cmHg]$
t	Time	$[s]$
W	Weight of membrane	$[g]$

Y_t	Yield of sericin at time t	[%]
Y_∞	Total sericin content	[%]
α	Selectivity	[−]
ΔH_s	Heat of sorption	$[J/mole]$

Appendix A Sample calculations

Gas permeability

The permeability of a gas can be calculated using equation (3.3):

$$P = \frac{Fl}{A\Delta p} \tag{3.3}$$

where P is the permeability, F is the permeation rate of the gas through the membrane, l and A are the thickness of the membrane and the area of permeation, respectively, and Δp is the pressure difference across the membrane.

For example, it took 5 min and 50 s for 0.1 mL of nitrogen to be transported through a membrane of thickness $0.003\,cm$ at $25^{\circ}C$ and 1 atm. The pressure difference across the membrane was 60 psi. The area of permeation was $15.2\,cm^2$. First, the permeate flow rate can be corrected to standard temperature and pressure (STP), based on ideal gas law

$$V_{STP} = V_{298K}\frac{T_{273K}}{T_{298K}} = 0.1cm^3 \times \frac{273K}{298K} = 0.092cm^3(STP)$$

The permeation rate of nitrogen (STP) is:

$$F_{N_2} = \frac{0.092cm^3(STP)}{350s} = 2.63\times10^{-4}cm^3(STP)/s$$

The permeability of nitrogen can be calculated to be:

$$P_{N_2} = \frac{F_{N_2}l}{A\Delta p_{N_2}} = \frac{2.63\times10^{-4}cm^3(STP)/s\times0.003cm}{15.2cm^2\times(60/14.696\times76cmHg)}$$

$$= 1.67\times10^{-10}cm^3(STP)\cdot cm/(cm^2\cdot s\cdot cmHg) = 1.67Barrer$$

If it took 1 min and 30 s for 1 mL of carbon dioxide to be transported through the same membrane at the same conditions, the permeability of carbon dioxide can be calculated.

$$V_{STP} = 1.0cm^3 \times \frac{273K}{298K} = 0.92cm^3(STP),$$

$$F_{CO_2} = \frac{0.92cm^3(STP)}{90s} = 1.02\times10^{-2}cm^3(STP)/s$$

$$P_{CO_2} = \frac{F_{CO_2}l}{A\Delta p_{CO_2}} = \frac{1.02\times10^{-2}cm^3(STP)/s\times0.003cm}{15.2cm^2\times(60/14.696\times76cmHg)}$$

$$= 6.0\times10^{-9}cm^3(STP)\cdot cm/(cm^2\cdot s\cdot cmHg) = 60Barrer$$

Membrane selectivity

The pure gas permeability ratio of carbon dioxide over nitrogen is calculated to be

$$\alpha_{CO_2/N_2} = \frac{P_{CO_2}}{P_{N_2}} = \frac{6.0\times10^{-9}}{1.67\times10^{-10}} = 35.9$$

Thus, the membrane selectivity is 35.9 for this example.

Appendix B Yield of sericin

Effect of extraction time on the yield of silk sericin [%] at different temperatures ($25 \sim 95^{\circ}C$), 1 atm

Temperature / Time	**25**$^{\circ}C$	**50**$^{\circ}C$	**75**$^{\circ}C$	**85**$^{\circ}C$	**95**$^{\circ}C$
0.1 hr	2.3	2.7	3.8	4.3	5.9
0.25 hr	3.1	3.5	4.2	5	9.6
0.5 hr	3.3	3.9	4.8	6.2	11.1
1 hr	3.4	4.7	5.5	8.4	14.2
3 hr	4.2	5.7	6.1	11.4	18.3
6 hr	4.7	6.4	7.3	15	21.7
9 hr	5.5	7.3	8.4	16.6	22.8

Effect of extraction temperature ($25 \sim 95^{\circ}C$) on the yield of silk sericin at different time (0.1~9 hr), 1 atm (Y_t / Y_{∞} vs temperature [$^{\circ}C$])

Temperature / Extraction Time	$25^{\circ}C$	$50^{\circ}C$	$75^{\circ}C$	$85^{\circ}C$	$95^{\circ}C$
0.1 hr	0.092	0.108	0.152	0.172	0.236
0.25 hr	0.124	0.14	0.168	0.2	0.384
0.5 hr	0.132	0.156	0.192	0.248	0.444
1 hr	0.136	0.188	0.22	0.336	0.568
3 hr	0.168	0.228	0.244	0.456	0.732
6 hr	0.188	0.256	0.292	0.6	0.868
9 hr	0.22	0.292	0.336	0.664	0.912

Appendix C Membrane Permeability

Permeability of Carbon dioxide (Figure 4-7)

Volume of gas permeate **2.75** cm^3

Operating temperature **298** K

Permeation area **15.2** cm^2

	Concentration of sericin in membrane							
	0% (Pure PVA)				**1.34%**			
Pressure differential [psi]	30	40	50	60	30	40	50	60
Time [s]	526.07	375.72	288.36	239.91	339.21	241.96	190.78	160.49
Thickness [*cm*]	0.003	0.003	0.003	0.003	0.0025	0.0025	0.0025	0.0025
Permeability [*Barrer*]	66.46	69.80	72.75	72.87	85.90	90.32	91.64	90.78

	Concentration of sericin in membrane							
	3.91%				**6.6%**			
Pressure differential [psi]	30	40	50	60	30	40	50	60
Time [s]	250.37	181.23	144.28	121.59	230.34	170.44	135.71	114.61
Thickness [*cm*]	0.0025	0.0025	0.0025	0.0025	0.0025	0.0025	0.0025	0.0025
Permeability [*Barrer*]	116.38	120.58	121.17	119.82	126.50	128.21	128.82	127.62
	9.92%				**15.68%**			
Pressure differential [psi]	30	40	50	60	30	40	50	60
Time [s]	243.37	174.98	139.91	116.71	193.84	142.59	113.85	96.5
Thickness [*cm*]	0.0025	0.0025	0.0025	0.0025	0.002	0.002	0.002	0.002
Permeability [*Barrer*]	119.72	124.89	124.95	124.83	120.25	122.61	122.84	120.78

	Concentration of sericin in membrane							
	21.50%				30.30%			
Pressure differential [psi]	30	40	50	60	30	40	50	60
Time [s]	241.73	177.66	141.44	118.38	266.35	194.55	150.89	127.88
Thickness [*cm*]	0.0025	0.0025	0.0025	0.0025	0.0025	0.0025	0.0025	0.0025
Permeability [*Barrer*]	120.54	123.00	123.60	123.07	109.39	112.33	115.86	113.92

Permeability of Nitrogen (Figure 4-8)

Volume of gas permeate **2.75** cm^3

Operating temperature **298** K

Permeation area **15.2** cm^2

	Concentration of sericin in membrane							
	0% (Pure PVA)				**1.34%**			
Pressure differential [psi]	30	40	50	60	30	40	50	60
Time [s]	2541.44	1948.06	1575.28	1337.57	1689.97	1299.05	1036.03	896.37
Thickness [*cm* **]**	0.003	0.003	0.003	0.003	0.0025	0.0025	0.0025	0.0025
Permeability [*Barrer* **]**	1.38	1.35	1.33	1.31	1.72	1.68	1.69	1.63

	Concentration of sericin in membrane							
	3.91%				**6.6%**			
Pressure differential [psi]	30	40	50	60	30	40	50	60
Time [s]	1334.28	1023.59	839.41	710.28	1247.04	948.16	783.34	661.68
Thickness [*cm*]	0.0025	0.0025	0.0025	0.0025	0.0025	0.0025	0.0025	0.0025
Permeability [*Barrer*]	2.18	2.13	2.08	2.05	2.34	2.30	2.23	2.20
	9.92%				**15.68%**			
Pressure differential [psi]	30	40	50	60	30	40	50	60
Time [s]	1336.56	1033.12	835.37	700.08	1024.06	804.52	659.47	552.97
Thickness [*cm*]	0.0025	0.0025	0.0025	0.0025	0.002	0.002	0.002	0.002
Permeability [*Barrer*]	2.18	2.12	2.09	2.08	2.28	2.17	2.12	2.11

	Concentration of sericin in membrane							
	21.50%				30.30%			
Pressure differential [psi]	30	40	50	60	30	40	50	60
Time [s]	1290.22	984.12	809.24	702.07	1443.37	1044.75	861.48	734.59
Thickness [*cm*]	0.0025	0.0025	0.0025	0.0025	0.0025	0.0025	0.0025	0.0025
Permeability [*Barrer*]	2.26	2.22	2.16	2.08	2.02	2.09	2.03	1.98

Permeability of Oxygen (Figure 4-9)

Volume of gas permeate **2.75** cm^3

Operating temperature **298** K

Permeation area **15.2** cm^2

	Concentration of sericin in membrane							
	0% (Pure PVA)				**1.34%**			
Pressure differential [psi]	30	40	50	60	30	40	50	60
Time [s]	1321.9	901.69	725.5	599.75	1154.07	802.49	633.64	517.47
Thickness [*cm*]	0.003	0.003	0.003	0.003	0.003	0.003	0.003	0.003
Permeability [*Barrer*]	2.65	2.91	2.89	2.91	3.03	3.27	3.31	3.38

	Concentration of sericin in membrane							
	3.91%				**6.6%**			
Pressure differential [psi]	30	40	50	60	30	40	50	60
Time [s]	633.56	459.51	355.25	301.69	750.21	564.38	433.38	365.36
Thickness [*cm*]	0.002	0.002	0.002	0.002	0.0025	0.0025	0.0025	0.0025
Permeability [*Barrer*]	3.68	3.80	3.94	3.86	3.88	3.87	4.03	3.99
	9.92%				**15.68%**			
Pressure differential [psi]	30	40	50	60	30	40	50	60
Time [s]	857.47	620.56	468.02	401.79	2033.31	1367.88	1035.91	858.38
Thickness [*cm*]	0.0025	0.0025	0.0025	0.0025	0.0055	0.0055	0.0055	0.0055
Permeability [*Barrer*]	3.40	3.52	3.74	3.63	3.15	3.51	3.71	3.73

	Concentration of sericin in membrane							
	21.50%				30.30%			
Pressure differential [psi]	30	40	50	60	30	40	50	60
Time [s]	1088.47	771.38	605.71	510.1	730.47	537.24	420.48	347.59
Thickness [*cm*]	0.003	0.003	0.003	0.003	0.002	0.002	0.002	0.002
Permeability [*Barrer*]	3.21	3.40	3.46	3.43	3.19	3.25	3.33	3.35

Appendix D Membrane Selectivity

Selectivity of carbon dioxide and nitrogen $[P_{CO_2} / P_{N_2}]$ **(Figure 4-10)**

Sericin concentration in membrane	Pressure difference across membrane [psi]			
	30	**40**	**50**	**60**
0% (Pure PVA)	48.31	51.85	54.63	55.75
1.34%	49.82	53.69	54.30	55.85
3.91%	53.29	56.48	58.18	58.42
6.6%	54.14	55.63	57.72	57.96
9.92%	54.92	59.04	59.71	59.98
15.68%	52.83	56.42	57.92	57.30
21.50%	53.37	55.39	57.21	59.31
30.30%	54.19	53.70	57.09	57.44

Selectivity of oxygen and nitrogen $[P_{O_2} / P_{N_2}]$ **(Figure 4-11)**

Sericin concentration in membrane	Pressure difference across membrane [psi]			
	30	**40**	**50**	**60**
0% Pure PVA	1.92	2.16	2.17	2.23
1.34%	1.76	1.94	1.96	2.08
3.91%	1.68	1.78	1.89	1.88
6.6%	1.66	1.68	1.81	1.81
9.92%	1.56	1.66	1.78	1.74
15.68%	1.39	1.62	1.75	1.77
21.50%	1.42	1.53	1.60	1.65
30.30%	1.58	1.56	1.64	1.69

Appendix E Degree of swelling of the membrane in water

Swelling ratio at 25$^{\circ}C$ (Figure 4-12)

Sericin concentration [%]	0	1.34	3.91	6.6	9.92	15.68	21.5	30.3
Swelling ratio [%]	106.14	113.59	130.28	152.08	139.60	144	141.81	144.10

Appendix F Water vapor sorption data

Water vapor sorption (at 25$^{\circ}C$, 1atm) in membranes with different content of sericin (Figure 4-13)

0% (Pure PVA)		1.34%	
M_t / M_∞	$t^{1/2} / l[s^{1/2}cm]$	M_t / M_∞	$t^{1/2} / l[s^{1/2}cm]$
0.00	0.00	0.00	0.00
0.08	10649.96	0.07	9797.96
0.08	15061.31	0.07	13856.41
0.17	21299.91	0.14	19595.92
0.17	26086.96	0.14	24000.00
0.17	31949.87	0.14	29393.88
0.25	45183.93	0.21	41569.22
0.33	58332.21	0.21	53665.63
0.33	78260.87	0.29	72000.00
0.42	133017.90	0.43	122376.47
0.50	149858.16	0.50	137869.50
0.50	182608.70	0.57	168000.00
0.58	200377.72	0.64	184347.50
0.58	225919.67	0.71	207846.10
0.67	234782.61	0.71	216000.00
0.75	292825.36	0.86	269399.33
0.83	344110.59	0.93	316581.74

3.91%		6.6%	
M_t / M_∞	$t^{1/2} / l[s^{1/2}cm]$	M_t / M_∞	$t^{1/2} / l[s^{1/2}cm]$
0.00	0.00	0.00	0.00
0.18	9797.96	0.10	8164.97
0.18	13856.41	0.10	11547.01
0.18	19595.92	0.10	16329.93
0.27	24000.00	0.10	20000.00
0.27	29393.88	0.20	24494.90
0.36	41569.22	0.30	34641.02
0.36	53665.63	0.30	44721.36
0.45	72000.00	0.40	60000.00
0.64	122376.47	0.70	101980.39
0.73	137869.50	0.80	114891.25
0.82	168000.00	0.90	140000.00
0.82	184347.50	1.00	153622.91
0.91	207846.10	1.00	173205.08
0.91	216000.00	1.00	180000.00
0.91	269399.33	1.00	224499.44
1.00	316581.74	1.00	263818.12

9.92%		15.68%	
M_t / M_∞	$t^{1/2} / l[s^{1/2}cm]$	M_t / M_∞	$t^{1/2} / l[s^{1/2}cm]$
0.00	0.00	0.00	0.00
0.09	9797.96	0.14	9797.96
0.18	13856.41	0.14	13856.41
0.27	19595.92	0.14	19595.92
0.27	24000.00	0.14	24000.00
0.27	29393.88	0.29	29393.88
0.36	41569.22	0.29	41569.22
0.45	53665.63	0.43	53665.63
0.45	72000.00	0.43	72000.00
0.73	122376.47	0.57	122376.47
0.82	137869.50	0.71	137869.50
0.91	168000.00	0.86	168000.00
0.91	184347.50	0.86	184347.50
0.91	207846.10	1.00	207846.10
1.00	216000.00	1.00	216000.00
1.00	269399.33	1.00	269399.33
1.00	316581.74	1.00	316581.74

21.50%		30.30%	
M_t / M_∞	$t^{1/2} / l[s^{1/2}cm]$	M_t / M_∞	$t^{1/2} / l[s^{1/2}cm]$
0.00	0.00	0.00	0.00
0.11	9797.96	0.00	9797.96
0.11	13856.41	0.10	13856.41
0.11	19595.92	0.10	19595.92
0.11	24000.00	0.20	24000.00
0.11	29393.88	0.30	29393.88
0.22	41569.22	0.30	41569.22
0.33	53665.63	0.30	53665.63
0.44	72000.00	0.40	72000.00
0.67	122376.47	0.70	122376.47
0.78	137869.50	0.80	137869.50
0.78	168000.00	0.90	168000.00
0.89	184347.50	0.90	184347.50
0.89	207846.10	0.90	207846.10
1.00	216000.00	1.00	216000.00
1.00	269399.33	1.00	269399.33
1.00	316581.74	1.00	316581.74

Appendix G Water vapor desorption data

Water vapor desorption (at 25$^{\circ}C$, 1atm) from pre-saturated membranes with different content of sericin (Figure 4-14)

0% (Pure PVA)			
M_t / M_∞	$t^{1/2} / l[s^{1/2}cm]$	M_t / M_∞	$t^{1/2} / l[s^{1/2}cm]$
0.00	0.00	0.57	16498.84
0.05	3367.81	0.59	16839.06
0.09	4762.80	0.61	17172.54
0.12	5833.22	0.62	17499.66
0.15	6735.62	0.64	17820.78
0.18	7530.66	0.66	18136.22
0.21	8249.42	0.67	18446.26
0.23	8910.39	0.69	18751.18
0.26	9525.61	0.70	19051.22
0.28	10103.43	0.71	19346.60
0.30	10649.96	0.73	19637.55
0.33	11169.77	0.74	19924.24
0.35	11666.44	0.76	20206.87
0.37	12142.82	0.77	20485.60
0.39	12601.20	0.78	20760.59
0.41	13043.48	0.79	21031.98
0.43	13471.25	0.81	21299.91
0.45	13885.84	0.83	21825.91
0.47	14288.41	0.85	22339.53
0.48	14679.95	0.87	23088.55
0.50	15061.31	0.89	23814.02
0.52	15433.25	0.91	24976.36
0.54	15796.44	0.93	26086.96
0.56	16151.46	0.97	36892.53

1.34%			
M_t / M_∞	$t^{1/2} / l[s^{1/2}cm]$	M_t / M_∞	$t^{1/2} / l[s^{1/2}cm]$
0.00	0.00	0.58	15178.93
0.03	3098.39	0.59	15491.93
0.06	4381.78	0.60	15798.73
0.09	5366.56	0.62	16099.69
0.12	6196.77	0.63	16395.12
0.14	6928.20	0.65	16685.32
0.17	7589.47	0.66	16970.56
0.20	8197.56	0.67	17251.09
0.23	8763.56	0.68	17527.12
0.26	9295.16	0.70	17798.88
0.29	9797.96	0.71	18066.54
0.32	10276.19	0.72	18330.30
0.35	10733.13	0.73	18590.32
0.37	11171.39	0.74	18846.75
0.40	11593.10	0.75	19099.74
0.41	12000.00	0.76	19349.42
0.44	12393.55	0.77	19595.92
0.46	12774.98	0.79	20079.84
0.48	13145.34	0.81	20552.37
0.50	13505.55	0.84	21241.47
0.51	13856.41	0.86	21908.90
0.53	14198.59	0.89	22978.25
0.55	14532.72	0.91	24000.00
0.56	14859.34	0.96	33941.13

3.91%			
M_t / M_∞	$t^{1/2} / l[s^{1/2}cm]$	M_t / M_∞	$t^{1/2} / l[s^{1/2}cm]$
0.00	0.00	0.57	15178.93
0.05	3098.39	0.59	15491.93
0.09	4381.78	0.61	15798.73
0.12	5366.56	0.62	16099.69
0.15	6196.77	0.64	16395.12
0.18	6928.20	0.65	16685.32
0.21	7589.47	0.67	16970.56
0.23	8197.56	0.68	17251.09
0.26	8763.56	0.69	17527.12
0.28	9295.16	0.71	17798.88
0.30	9797.96	0.72	18066.54
0.32	10276.19	0.73	18330.30
0.35	10733.13	0.74	18590.32
0.37	11171.39	0.75	18846.75
0.39	11593.10	0.77	19099.74
0.41	12000.00	0.78	19349.42
0.43	12393.55	0.79	19595.92
0.45	12774.98	0.80	20079.84
0.47	13145.34	0.82	20552.37
0.49	13505.55	0.85	21241.47
0.50	13856.41	0.86	21908.90
0.52	14198.59	0.89	22978.25
0.54	14532.72	0.92	24000.00
0.56	14859.34	0.97	33941.13

6.6%			
M_t / M_∞	$t^{1/2} / l[s^{1/2}cm]$	M_t / M_∞	$t^{1/2} / l[s^{1/2}cm]$
0.00	0.00	0.53	12649.11
0.03	2581.99	0.55	12909.94
0.06	3651.48	0.57	13165.61
0.09	4472.14	0.58	13416.41
0.12	5163.98	0.60	13662.60
0.14	5773.50	0.62	13904.44
0.17	6324.56	0.63	14142.14
0.19	6831.30	0.64	14375.91
0.22	7302.97	0.66	14605.93
0.24	7745.97	0.67	14832.40
0.26	8164.97	0.68	15055.45
0.29	8563.49	0.70	15275.25
0.31	8944.27	0.71	15491.93
0.33	9309.49	0.73	15705.63
0.35	9660.92	0.74	15916.45
0.37	10000.00	0.75	16124.52
0.39	10327.96	0.76	16329.93
0.41	10645.81	0.78	16733.20
0.43	10954.45	0.81	17126.98
0.45	11254.63	0.84	17701.22
0.47	11547.01	0.86	18257.42
0.49	11832.16	0.90	19148.54
0.50	12110.60	0.93	20000.00
0.52	12382.78	1.00	28284.27

15.68%			
M_t / M_∞	$t^{1/2} / l[s^{1/2}cm]$	M_t / M_∞	$t^{1/2} / l[s^{1/2}cm]$
0.00	0.00	0.66	15178.93
0.05	3098.39	0.68	15491.93
0.08	4381.78	0.69	15798.73
0.12	5366.56	0.71	16099.69
0.14	6196.77	0.73	16395.12
0.18	6928.20	0.74	16685.32
0.21	7589.47	0.75	16970.56
0.24	8197.56	0.76	17251.09
0.27	8763.56	0.77	17527.12
0.31	9295.16	0.78	17798.88
0.35	9797.96	0.79	18066.54
0.38	10276.19	0.80	18330.30
0.42	10733.13	0.81	18590.32
0.44	11171.39	0.82	18846.75
0.47	11593.10	0.82	19099.74
0.49	12000.00	0.83	19349.42
0.51	12393.55	0.84	19595.92
0.53	12774.98	0.84	20079.84
0.56	13145.34	0.85	20552.37
0.57	13505.55	0.86	21241.47
0.59	13856.41	0.87	21908.90
0.61	14198.59	0.88	22978.25
0.63	14532.72	0.89	24000.00
0.64	14859.34	0.90	33941.13

21.5%			
M_t / M_∞	$t^{1/2} / l[s^{1/2}cm]$	M_t / M_∞	$t^{1/2} / l[s^{1/2}cm]$
0.00	0.00	0.61	15178.93
0.04	3098.39	0.63	15491.93
0.08	4381.78	0.65	15798.73
0.11	5366.56	0.66	16099.69
0.15	6196.77	0.68	16395.12
0.17	6928.20	0.70	16685.32
0.20	7589.47	0.72	16970.56
0.23	8197.56	0.74	17251.09
0.26	8763.56	0.75	17527.12
0.29	9295.16	0.77	17798.88
0.31	9797.96	0.78	18066.54
0.33	10276.19	0.80	18330.30
0.35	10733.13	0.81	18590.32
0.37	11171.39	0.83	18846.75
0.39	11593.10	0.84	19099.74
0.42	12000.00	0.85	19349.42
0.44	12393.55	0.86	19595.92
0.46	12774.98	0.88	20079.84
0.49	13145.34	0.90	20552.37
0.51	13505.55	0.92	21241.47
0.53	13856.41	0.93	21908.90
0.55	14198.59	0.95	22978.25
0.57	14532.72	0.95	24000.00
0.59	14859.34	0.99	33941.13

30.3%			
M_t / M_∞	$t^{1/2} / l[s^{1/2}cm]$	M_t / M_∞	$t^{1/2} / l[s^{1/2}cm]$
0.00	0.00	0.56	14054.57
0.03	2868.88	0.58	14344.38
0.06	4057.20	0.60	14628.46
0.10	4969.04	0.61	14907.12
0.13	5737.75	0.62	15180.67
0.16	6415.00	0.64	15449.37
0.19	7027.28	0.65	15713.48
0.22	7590.33	0.67	15973.23
0.24	8114.41	0.68	16228.82
0.27	8606.63	0.69	16480.44
0.29	9072.18	0.71	16728.28
0.32	9514.99	0.72	16972.50
0.34	9938.08	0.72	17213.26
0.36	10343.88	0.74	17450.69
0.38	10734.35	0.75	17684.94
0.40	11111.11	0.76	17916.13
0.42	11475.51	0.77	18144.37
0.44	11828.68	0.79	18592.45
0.46	12171.61	0.81	19029.97
0.48	12505.14	0.83	19668.03
0.49	12830.01	0.85	20286.02
0.51	13146.84	0.88	21276.16
0.53	13456.22	0.91	22222.22
0.55	13758.65	1.00	31426.97

Appendix H Diffusion coefficient

Diffusion coefficient determined from sorption and desorption experiments at 25$^{\circ}C$, 1atm (Figure 4-16)

Sericin concentration in membrane [%]	$D_s[cm^2/s]$	$D_d[cm^2/s]$
0	1.699E-12	2.534E-10
1.34	2.488E-12	2.852E-10
3.91	2.488E-12	2.923E-10
6.6	1.068E-12	3.770E-10
15.68	6.413E-12	3.631E-10
21.5	6.075E-12	3.368E-10
30.3	8.319E-12	3.258E-10

Appendix I Sample of polymath report

- Polymath report for water vapor sorption coefficient in 6.6% of sericin contents in membrane

POLYMATH Results
No Title 05-11-2007

Nonlinear regression (L-M)

Model: M = 1-0.81057*exp(-A*t)-1/9*0.81057*exp(-9*A*t) -1/25*0.81057*exp(-25*A*t) -1/49*0.81057*exp(-49*A*t) -1/81*0.81057*exp(-81*A*t)-1/121*0.81057*exp(-121*A*t)-1/169*0.81057*exp(-169*A*t)-1/225*0.81057*exp(-225*A*t)-1/289*0.81057*exp(-289*A*t)-1/361*0.81057*exp(-361*A*t)-1/441*0.81057*exp(-441*A*t)-1/529*0.81057*exp(-529*A*t)-1/625*0.81057*exp(-625*A*t)

Variable	Ini guess	Value	95% confidence
A	1.0E-06	1.172E-05	4.203E-10

Nonlinear regression settings
Max # iterations = 64

Precision
R^2 = 0.9934242
R^2adj = 0.9934242
Rmsd = 0.0076846
Variance = 0.0010666

General
Sample size = 17
Model vars = 1
Indep vars = 1
Iterations = 8

Note: $M = \frac{M_t}{M_\infty}$ and $A = \frac{\pi^2}{l^2} D$

Water vapor sorption (at 25$^{\circ}C$, 1atm) in membranes with 6.6% of sericin

6.6%	
M_t / M_∞	$t[s]$
0.00	0
0.10	600
0.10	1200
0.10	2400
0.10	3600
0.20	5400
0.30	10800
0.30	18000
0.40	32400
0.70	93600
0.80	118800
0.90	176400
1.00	212400
1.00	270000
1.00	291600
1.00	453600
1.00	626400

POLYMATH Results

POLYMATH Report 05-11-2007, Rev5.1.225

Explicit Algebraic Equations Solution

Variable	Value
t	200
A	1.172E-05
M	0.0353603
L	0.003
D	1.069E-11

Explicit Algebraic Equations Report

Explicit equations

[1] t = 200

[2] A = 1.172E-05

[3] M = 1-0.81057*exp(-A*t)-1/9*0.81057*exp(-9*A*t) -1/25*0.81057*exp(-25*A*t) -1/49*0.81057*exp(-49*A*t) -1/81*0.81057*exp(-81*A*t)-1/121*0.81057*exp(-121*A*t)-1/169*0.81057*exp(-169*A*t)-1/225*0.81057*exp(-225*A*t)-1/289*0.81057*exp(-289*A*t)-1/361*0.81057*exp(-361*A*t)-1/441*0.81057*exp(-441*A*t)-1/529*0.81057*exp(-529*A*t)-1/625*0.81057*exp(-625*A*t)

[4] L = 0.003

[5] D = A*L^2/3.14159/3.14159

General

number of implicit equations: 0

number of explicit equations: 5

Data file: \\ecfile1\sj2kim\My Documents\My eBooks\6.61% sorption(D) report.pol

---

Note: $D = \frac{A \cdot l^2}{\pi^2}$

- Polymath report for water vapor desorption coefficient in 6.6% of sericin contents in membrane

POLYMATH Results
No Title 05-11-2007

Nonlinear regression (L-M)

Model: M = 1-0.81057*exp(-A*t)-1/9*0.81057*exp(-9*A*t) -1/25*0.81057*exp(-25*A*t) -1/49*0.81057*exp(-49*A*t) -1/81*0.81057*exp(-81*A*t)-1/121*0.81057*exp(-121*A*t)-1/169*0.81057*exp(-169*A*t)-1/225*0.81057*exp(-225*A*t)-1/289*0.81057*exp(-289*A*t)-1/361*0.81057*exp(-361*A*t)-1/441*0.81057*exp(-441*A*t)-1/529*0.81057*exp(-529*A*t)-1/625*0.81057*exp(-625*A*t)

Variable	Ini guess	Value	95% confidence
A	1.0E-06	4.134E-04	3.382E-05

Nonlinear regression settings
Max # iterations = 64

Precision
R^2 = 0.9292545
R^2adj = 0.9292545
Rmsd = 0.0099179
Variance = 0.0048219

General
Sample size = 48
Model vars = 1
Indep vars = 1
Iterations = 7

Note: $M = \frac{M_t}{M_\infty}$ and $A = \frac{\pi^2}{l^2} D$

Water vapor desorption (at 25$^{\circ}C$, 1atm) from pre-saturated membranes with 6.6% of sericin

6.6%			
M_t / M_∞	$t[s]$	M_t / M_∞	$t[s]$
0.00	0	0.53	1440
0.03	60	0.55	1500
0.06	120	0.57	1560
0.09	180	0.58	1620
0.12	240	0.60	1680
0.14	300	0.62	1740
0.17	360	0.63	1800
0.19	420	0.64	1860
0.22	480	0.66	1920
0.24	540	0.67	1980
0.26	600	0.68	2040
0.29	660	0.70	2100
0.31	720	0.71	2160
0.33	780	0.73	2220
0.35	840	0.74	2280
0.37	900	0.75	2340
0.39	960	0.76	2400
0.41	1020	0.78	2520
0.43	1080	0.81	2640
0.45	1140	0.84	2820
0.47	1200	0.86	3000
0.49	1260	0.90	3300
0.50	1320	0.93	3600
0.52	1380	1.00	7200

POLYMATH Results

POLYMATH Report 05-11-2007, Rev5.1.225

Explicit Algebraic Equations Solution

Variable	Value
t	200
A	4.134E-04
M	0.2065543
L	0.003
D	3.77E-10

Explicit Algebraic Equations Report

Explicit equations

[1] t = 200

[2] A = 4.134E-04

[3] M = 1-0.81057*exp(-A*t)-1/9*0.81057*exp(-9*A*t) -1/25*0.81057*exp(-25*A*t) -1/49*0.81057*exp(-49*A*t) -1/81*0.81057*exp(-81*A*t)-1/121*0.81057*exp(-121*A*t)-1/169*0.81057*exp(-169*A*t)-1/225*0.81057*exp(-225*A*t)-1/289*0.81057*exp(-289*A*t)-1/361*0.81057*exp(-361*A*t)-1/441*0.81057*exp(-441*A*t)-1/529*0.81057*exp(-529*A*t)-1/625*0.81057*exp(-625*A*t)

[4] L = 0.003

[5] D = A*L^2/3.14159/3.14159

General

number of implicit equations: 0

number of explicit equations: 5

Data file: \\ecfile1\sj2kim\My Documents\My eBooks\6.61% desorption(D).pol

---

Note: $D = \frac{A \cdot l^2}{\pi^2}$